DESIGN OF BEAMS WITH ECCENTRIC REINFORCED WEB OPENINGS

by

ROBERT JEN-PING SAND

B.S., National Taiwan University, 1971

A MASTER'S REPORT

submitted in partial fulfillment of the

requirement for the degree

MASTER OF SCIENCE

Department of Civil Engineering

KANSAS STATE UNIVERSITY
Manhattan, Kansas

1977

Approved by:

Major professor

TABLE OF CONTENTS

THIS BOOK CONTAINS NUMEROUS PAGES WITH DIAGRAMS THAT ARE CROOKED COMPARED TO THE REST OF THE INFORMATION ON THE PAGE.

THIS IS AS RECEIVED FROM CUSTOMER.

TABLE OF CONTENTS(Continued)

LIST OF TABLES

LIST OF FIGURES

INTRODUCTION

In modern buildings, many ducts for heating, ventilation, and air conditioning systems will be placed within the building. For multi-story buildings, it is more economical to pass these ducts through floor beams rather than under them. Not only does this practice save in the overall height of the structure along with all the related benefits in material savings, but it also saves in the cost of heating and air-conditioning because the enclosed volume is less. Since not all floor beams and girders are of same depth at any given floor level, eccentric openings are unavoidable, and sometimes the addition of reinforcement is desirable so that with the opening a heavier section is not required. In the past few years considerable effort has been made to develop theoretical and experimental information on steel beams with web openings.

For the case of beams with unreinforced and reinforced concentric rectangular web opening, a suggested design guide (1) is available. Also a design guide (2) has been published for beams with eccentric circular web openings. Bower (3) developed elastic design curves for beams with concentric circular and rectangular web openings and Douglas and Gambrell (4) followed his procedures to present elastic design curves for beams with eccentric rectangular openings. However, neither of these articles consider adding reinforcement around the opening. Plastic design curves for concentric and eccentric rectangular openings with reinforcement were developed by Wang, Snell and Cooper (5). This report presents elastic design curves for eccentric rectangular web openings with specific amounts of reinforcement. The reinforcing consists of straight rectangular bars welded to the web just above and below the web opening on one or both side of the beam.

Part I of this report deals with the justification of a commonly used

equation for calculating stresses in beams with web openings. In Part II yield equations are derived and the design curves for certain sections are plotted for use as a design guide. In Part III an example problem is presented to illustrate the use of the design curves in the design of a building floor system.

Although the plastic design method has been recommended by many engineers as the more rational approach to designing steel members, there is little to be gained by applying the plastic design method to statically determinate structures, and for high strength steels, only the elastic design method is permitted by AISC. Hence the elastic design procedure is often still used.

PART I : JUSTIFICATION OF VIERENDEEL METHOD OF ANALYSIS

Vierendeel Equation

The Vierendeel method of analysis was originally developed for rigid concrete trusses with posts normal to the main longitudinal chords of the truss. It was later used for rigid steel trusses of the same type. This approximate elastic analysis, when applied to beams with rectangular web openings, predicts quite accurately the stresses in the vincinity of the opening. But this method has its limitations, first it can only be applied to rectangular web openings, and second it does not account for the stress concentrations at the corners of the openings. For its application to beams with web openings, the following assumptions are made:

(1) The beam sections above and below the opening are fixed at their ends.

(2) Points of inflection occur in the sections at the vertical certerline of the opening.

(3) The amount of shearing force distributed to the sections above and below the opening must be assumed.

The Vierendeel method of analysis estimates the normal stresses at the opening as a summation of the primary bending stresses and a secondary bending stresses (Vierendeel stresses). The primary bending stresses are due to the bending moment at the centerline of the opening, while the secondary bending stresses are due to the shearing forces carried by the T-sections above and below the opening. The normal stress in the top section according to the Vierendeel method of analysis may be expressed as

$$f_T = \frac{M_o \cdot y_n}{I_n} + \frac{V_T \cdot x_o \cdot y_T}{I_T} \qquad (1a)$$

and the normal stress in the bottom section is

$$f_B = \frac{(M_o)(y_n)}{I_n} + \frac{(V_B)(x_o)(y_B)}{I_B} \qquad (1b)$$

where M_o = primary bending moment at the vertical centerline of the opening;

y_n = distance from neutral axis of the net beam section to any fiber, and is measured positive down;

V_T , V_B = shear in the top and bottom sections, respectively;

x_o = distance from the centerline of the opening, and measured positive toward the load;

y_T , y_B = distance from the neutral axis of the top and bottom sections to any fiber in the section, respectively, measured positive down;

I_T , I_B = moment of inertia of the top and bottom section, respectively.

Shear Distribution Ratio

Consideration of Eqs. (1) shows that the shear distribution ratio V_T/V_B must be known before the Vierendeel method of analysis can be applied. In the case of beams with concentric web openings, the value of V_T/V_B is one, but the ratio is different for beams with eccentric web openings.

To determine the shear distribution ratio V_T/V_B, three methods have been developed, which use the following general form:

$$\frac{V_T}{V_B} = \frac{\dfrac{a^2}{3I_B E/G} + \dfrac{K_B}{A_B}}{\dfrac{a^2}{3I_T E/G} + \dfrac{K_T}{A_T}} \qquad (2)$$

where a = one-half the opening width;

A = cross-sectional area;

I = moment of inertia;

K = shear deflection coefficient;

E = modulus of elasticity;

G = shear modulus = E/2(1+V);

V = Poisson's ratio;

T , B = subscripts referring to top and bottom sections, respectively.

This equation considers both shearing and bending deflections and is derived by equating the deflections of the T-sections above and below the opening.

The three methods of using Eq. (2) differ only in the shear deflection coefficient used. One method uses a shear deflection coefficient K which was derived on the basis of strain energy. The derivation of the equation for this coefficient is presented in Ahmad's Thesis (6). Douglas and Gambrell (4) suggest using the shear deflection coefficient K equal to 1/R, where R is the shear coefficient defined by Cowper (7). The equation presented by Frost (8) uses only the web area of the T-sections, along with the shear deflection coefficient for a rectangle of 1.2.

A comparison of the results of these three methods to those obtained from experimental and finite element strain data are presented by Ahmad (6), where the conclusion is reached that the strain energy derived shear deflection coefficient gave the best results, but that Frost's form of Eq. (2) was also satisfactory. Since Frost's method gives satisfactory results and is easier to apply than the other methods, it is used in this report. Frost's equation may be expressed as

$$\frac{V_T}{V_B} = \frac{\dfrac{a^2}{3I_B E/G} + \dfrac{1.2}{A_{WB}}}{\dfrac{a^2}{3I_T E/G} + \dfrac{1.2}{A_{WT}}} \qquad (3)$$

where A_{WT} = web area of top T-section = $t_W(d_T-t_f)$;

A_{WB} = web area of bottom T-section = $t_W(d_B-t_f)$;

$E/G = 2(1+\nu)$ where ν = Poisson's ratio.

Justification of Vierendeel Method of Analysis

In an attempt to justify the Vierendeel method of analysis, theoretical normal stresses given by Eq. (1) with the shear distribution ratio given by Eq. (3) are compared to experimental results from tests performed at Kansas State University. In order to obtain results which are independent of the load, the normal stress f is divided by the shearing force V in the section. From Eqs. (1) for the top section

$$\frac{f_T}{V} = \frac{M_o}{V} \cdot \frac{y_n}{I_n} + \frac{V_T}{V} \cdot \frac{(x_o)(y_T)}{I_T} \qquad (4a)$$

and for the bottom section

$$\frac{f_B}{V} = \frac{M_o}{V} \cdot \frac{y_n}{I_n} + \frac{V_B}{V} \cdot \frac{(x_o)(y_B)}{I_B} \qquad (4b)$$

The tests performed at Kansas State University dealt with W16 x 45 and W16 x 40 steel beams. All beams were simply supported and subjected to a single concentrated load at mid-span. The two W16 x 45 beams had 9" wide by 6" deep rectangular openings which were located 2 in. above the mid-depth and the vertical centerlines were 24 in. from the load point. Beam 1 was unreinforced whereas Beam 2 was reinforced. The beams were each tested at four different moment to shear ratios (M/V = 20, 40, 60, 80 in.).

The W16 x 40 beams had four different opening configurations, which were designated Beams 3,4,5, and 5a. All four beams had 12" wide by 9" deep rectangular openings which were located 2 in. from the mid-depth, and the vertical

centerline was 25 in. from the load point. The beams only differed in the amount of reinforcement used or in the eccentricity of the opening. The beams were each tested at three different moment to shear ratios (M/V = 20, 40, 60 in.).

The tests were conducted in a 200,000 lb. capacity, Tinius-Olsen screw type machine, with a lever-type load measuring system. The strain data was measured at sections 1-1/2 inches away from the edge of the opening by using linear electrical resistance strain gages. The stresses were obtained from the measured strains by multiplying by the modulus of elasticity E.

The loading condition and the sections at the opening where the strains were measured are shown in Fig. 1, these sections are referred to as the low moment section (LMS) and high moment section (HMS). The general cross section of the beams at the opening is shown in Fig. 2 and the dimensions are tabulated in Table 1.

The experimental normal stresses of these six test beams are presented in Table 2 through Table 7. These tables give the normal stresses at the eight critical sections shown in Fig. 1. By using Eq. (4) along with the shear distribution ratio determined by Eq. (3), and taking Poisson's ratio equal to 0.3, the theoretical values of f/V were calculated and are also shown in Table 2 through Table 7.

Comparing the experimental data to the theoretical values shows that at points of high stress, such as at extreme fibers at the high moment section, there is an average percent difference of 4.19%. Another point of high stress is the upper edge of the opening at the low moment section. The results for this point do not appear to be as good as that for the extreme fibers and are much worse for Beam 4 than the others. For all beams the average percent difference for this point is 15.59%. The percent difference was found as the

difference between the two stresses divided by the experimental value. These results are presented in Table 2 through Table 7.

PART II : ELASTIC DESIGN CRITERIA

von Mises Theory

The theory of yielding for steel that agrees most closely with experimental results is the von Mises theory. For the stresses at a point in the web of a beam, this theory can be simplified and written in the form

$$f_b^2 + 3 f_v^2 = F_y^2 \tag{5}$$

where f_b is the bending stress, f_v is the shearing stress and F_y is the yield stress of steel.

The AISC allowable stresses for the elastic design of beams are expressed in terms of the specified minimum tensile yield point of the steel F_y. Although there are many conditions for which the allowable stress may be slightly modified, the basic maximum allowable bending stress, F_b in noncompact rolled shapes, built-up members, and plate girders is

$$F_b = 0.6 F_y \tag{6}$$

and the basic allowable shearing stress F_v is

$$F_v = 0.4 F_y \tag{7}$$

If F_y is eliminated from Eq. (5) by using the relationships in Eqs. (6) and (7), the von Mises yield criteria may be written as

$$\left(\frac{f_b}{F_b}\right)^2 + \frac{4}{3}\left(\frac{f_v}{F_v}\right)^2 = \frac{25}{9} \tag{8}$$

In computing stresses in beams with web openings, the notations f_{bn} and f_{vn} are used instead of f_b and f_v, and Eq. (8) becomes

$$\left(\frac{f_{bn}}{F_b}\right)^2 + \frac{4}{3}\left(\frac{f_{vn}}{F_v}\right)^2 = \frac{25}{9} \tag{9}$$

In the investigation of stresses at openings in this report, the approximate Vierendeel Eqs. (1) are used to find the bending stresses. The shearing stresses f_{vn} are taken as the average stress in the web of the T-section and are written as V_T / A_{WT} and V_B / A_{WB} for the top and bottom sections, respectively.

It is probably more convenient for design purpose, however, to develop the yield equations in terms of the maximum nominal stresses that would occur in the web at the location of the opening if the opening were not present, since these latter stresses are the ones ordinary computed by designers. If the maximum nominal stresses for the gross section are denoted as f_{bg} for bending and f_{vg} for shear, Eq. (9) may be written as

$$A^2\left(\frac{f_{bg}}{F_b}\right)^2 + \frac{4}{3}B^2\left(\frac{f_{vg}}{F_v}\right)^2 = \frac{25}{9} \qquad (10)$$

where $A = f_{bn}/f_{bg}$ and $B = f_{vn}/f_{vg}$.

Yield Equations

For beams without web openings the extreme fibers of the section will govern the design, but for beams with web openings the stresses at the edges of the opening and at the interfaces of the web and flange must also be checked. The twelve points investigated are shown in Fig. 3.

For points at the edges of the opening and at the extreme fibers of the section where f_{vn} is equal to zero, i.e. at points 1,3,4,6,7,9,10,12, Eq.(10) reduces to

$$A\left(\frac{f_{bg}}{F_b}\right) = \pm\frac{5}{3} \qquad (11)$$

where the sign used depends upon the point being considered.

The coefficient A in Eq. (11) varies over the cross-section and must be derived for each point studied. As an example of the derivation procedures consider point 3. By using the flexure formula the bending stress at extreme fibers for the gross section may be written as

$$f_{bg} = \frac{Mo\ (d/2)}{I_g} \tag{12}$$

where d is the depth of the beam, and I_g is the moment of inertia of the gross section.

The shearing stress in the gross section is taken as

$$f_{vg} = \frac{V}{A_W} \tag{13}$$

where V is the shear force and A_W is the web area, which is equal to $d \cdot t_w$.

Substituting for the coefficient A in Eq. (11) and selecting the negative sign to correspond to the compression at this point, the yield equation becomes

$$\left(\frac{f_{bn}}{f_{bg}} \right) \left(\frac{f_{bg}}{F_b} \right) = -\frac{5}{3} \tag{14}$$

From Eq. (1a), f_{bn} for point 3 may be written as

$$f_{bn} = \frac{-M_o(\bar{y} - d_T)}{I_n} + \frac{V_T\ (-a)\ (y_3)}{I_T} \tag{15}$$

where $\bar{y}$ is the distance from the centroid of the net section to the top fiber, d_T is the depth of the top T-section, a is one-half the width of the opening and y_3 is the distance from the centroid of the top section to point 3.

Substituting Eqs. (12) and (15) into Eq. (14) gives

$$\frac{-2(\bar{y} - d_T)}{d} \cdot \frac{I_g}{I_n} \cdot \frac{f_{bg}}{F_b} + \frac{(V_T)(-a)(y_3)}{I_T \quad F_b} = -\frac{5}{3} \tag{16}$$

Eliminating F_y from Eqs. (6) and (7),

$$F_b = \frac{3}{2} F_v \tag{17}$$

Then by multiplying both numerator and denominator of the second term in Eq.(16) by V and A_w and making use of Eq. (17)

$$\frac{2(\bar{y} - d_T)}{d} \cdot \frac{I_g}{I_n} \cdot \frac{f_{bg}}{F_b} + \frac{2}{3} \cdot \frac{V_T}{V} \cdot \frac{V}{A_W} \cdot \frac{(a)(A_W)(y_3)}{I_T \quad F_v} = \frac{5}{3} \tag{18}$$

Now substituting f_{vg} for V/A_W into Eq. (18), the desired form of the yield equation for point 3 becomes

$$\frac{2(\bar{y} - d_T)}{d} \cdot \frac{I_g}{I_n} \cdot \frac{f_{bg}}{F_b} + \frac{2}{3} \cdot \frac{V_T}{V} \cdot \frac{(a)(A_W)(y_3)}{I_T} \cdot \frac{f_{vg}}{F_v} = \frac{5}{3} \tag{19a}$$

By using the notations shown in Fig.3 and Fig. 4 and following the same procedures as above, the yield equations were obtained for the other points:

For point 1

$$\frac{2\bar{y}}{d} \cdot \frac{I_g}{I_n} \cdot \frac{f_{bg}}{F_b} - \frac{2}{3} \cdot \frac{V_T}{V} \cdot \frac{(a)(A_W)(y_1)}{I_T} \cdot \frac{f_{vg}}{F_v} = \frac{5}{3} \tag{19b}$$

For point 4

$$\frac{2(d - \bar{y} - d_B)}{d} \cdot \frac{I_g}{I_n} \cdot \frac{f_{bg}}{F_b} + \frac{2}{3} \cdot \frac{V_B}{V} \cdot \frac{(a)(A_W)(y_4)}{I_B} \cdot \frac{f_{vg}}{F_v} = \frac{5}{3} \tag{19c}$$

For point 6

$$\frac{2(d-\bar{y})}{d}\cdot\frac{I_g}{I_n}\cdot\frac{f_{bg}}{F_b}-\frac{2}{3}\cdot\frac{V_B}{V}\cdot\frac{(a)(A_W)(y_6)}{I_B}\cdot\frac{f_{vg}}{F_v}=\frac{5}{3} \qquad (19d)$$

For point 7

$$\frac{2\bar{y}}{d}\cdot\frac{I_g}{I_n}\cdot\frac{f_{bg}}{F_b}+\frac{2}{3}\cdot\frac{V_T}{V}\cdot\frac{(a)(A_W)(y_1)}{I_T}\cdot\frac{f_{vg}}{F_v}=\frac{5}{3} \qquad (19e)$$

For point 9

$$\frac{2(\bar{y}-d_T)}{d}\cdot\frac{I_g}{I_n}\cdot\frac{f_{bg}}{F_b}-\frac{2}{3}\cdot\frac{V_T}{V}\cdot\frac{(a)(A_W)(y_3)}{I_T}\cdot\frac{f_{vg}}{F_v}=\frac{5}{3} \qquad (19f)$$

For point 10

$$\frac{2(d-\bar{y}-d_B)}{d}\cdot\frac{I_g}{I_n}\cdot\frac{f_{bg}}{F_b}-\frac{2}{3}\cdot\frac{V_B}{V}\cdot\frac{(a)(A_W)(y_4)}{I_B}\cdot\frac{f_{vg}}{F_v}=\frac{5}{3} \qquad (19g)$$

For point 12

$$\frac{2(d-\bar{y})}{d}\cdot\frac{I_g}{I_n}\cdot\frac{f_{bg}}{F_b}+\frac{2}{3}\cdot\frac{V_B}{V}\cdot\frac{(a)(A_W)(y_6)}{I_B}\cdot\frac{f_{vg}}{F_v}=\frac{5}{3} \qquad (19h)$$

For points at the interface of the web and flange, f_{vn} is not equal to zero. The second term in Eq. (10) as calculated for points in the top section may be written as

$$B\left(\frac{f_{vg}}{F_v}\right)=\frac{V_T}{V}\cdot\frac{A_W}{A_{WT}}\cdot\frac{f_{vg}}{F_v}$$

$$=\frac{V_T}{V}\cdot\frac{(d)(t_w)}{(d_T-t_f)t_w}\cdot\frac{f_{vg}}{F_v}$$

$$=\frac{V_T}{V}\cdot\frac{d}{(d_T-t_f)}\cdot\frac{f_{vg}}{F_v} \qquad (20a)$$

and for points in the bottom section as

$$B\left(\frac{f_{vg}}{F_v}\right) = \frac{V_B}{V} \cdot \frac{d}{(d_B - t_f)} \cdot \frac{f_{vg}}{F_v} \qquad (20b)$$

By substituting Eq. (20a) or Eq. (20b) for the second term in Eq. (10) and using the same procedures as before for the first term, we can obtain the yield equations for the points at the interface of the web and flange.

For point 2 we obtain

$$A\left(\frac{f_{bg}}{F_b}\right) = \frac{2(\bar{y} - t_f)}{d} \cdot \frac{I_g}{I_n} \cdot \frac{f_{bg}}{F_b} - \frac{2}{3} \cdot \frac{V_T}{V} \cdot \frac{(a)(A_W)(y_2)}{I_T} \cdot \frac{f_{vg}}{F_v}$$

and

$$B\left(\frac{f_{vg}}{F_v}\right) = \frac{V_T}{V} \cdot \frac{d}{(d_T - t_f)} \cdot \frac{f_{vg}}{F_v}$$

Then substituting these terms into Eq. (10), the yield equation becomes

$$\frac{4(\bar{y} - t_f)^2}{d^2}\left(\frac{I_g}{I_n}\right)^2\left(\frac{f_{bg}}{F_b}\right)^2 - \frac{8}{3} \cdot \frac{V_T}{V} \cdot \frac{(\bar{y} - t_f)}{d} \cdot \frac{I_g}{I_n} \cdot \frac{(A_W)(a)(y_3)}{I_T} \cdot \frac{f_{vg}}{F_v} \cdot \frac{f_{bg}}{F_b}$$

$$+ \left[\left(\frac{2A_W\, a\, y_2}{3I_T}\right)^2 + \frac{4}{3} \cdot \frac{d^2}{(d_T - t_f)^2}\right]\left(\frac{V_T}{V}\right)^2\left(\frac{f_{vg}}{F_v}\right)^2 = \frac{25}{9} \qquad (21a)$$

The equations for the other points at the interface of the web and flange, which were obtained by the same procedures, are as follows :

For point 5

$$\frac{4(d-\bar{y}-t_f)^2}{d^2}\left(\frac{I_g}{I_n}\right)^2\left(\frac{f_{bg}}{F_b}\right)^2 - \frac{8}{3} \cdot \frac{(d-\bar{y}-t_f)}{d} \cdot \frac{I_g}{I_n} \cdot \frac{(A_W)(a)(y_5)}{I_B} \cdot \frac{f_{vg}}{F_v} \cdot \frac{f_{bg}}{F_b}$$

$$+ \left[\left(\frac{2A_W\, a\, y_5}{3I_B}\right)^2 + \frac{4}{3} \cdot \frac{d^2}{(d_B - t_f)^2}\right]\left(\frac{V_B}{V}\right)^2\left(\frac{f_{vg}}{F_v}\right)^2 = \frac{25}{9} \qquad (21b)$$

For point 8

$$\frac{4(\bar{y} - t_f)^2}{d^2}\left(\frac{I_g}{I_n}\right)^2\left(\frac{f_{bg}}{F_b}\right)^2 + \frac{8}{3}\cdot\frac{V_T}{V}\cdot\frac{(\bar{y} - t_f)}{d}\cdot\frac{I_g}{I_n}\cdot\frac{(A_W)(a)(y_2)}{I_T}\cdot\frac{f_{vg}}{F_v}\cdot\frac{f_{bg}}{F_b}$$

$$+\left[\left(\frac{2A_W\, a\, y_2}{3I_T}\right)^2 + \frac{4}{3}\cdot\frac{d^2}{(d_T - t_f)^2}\right]\left(\frac{V_T}{V}\right)^2\left(\frac{f_{vg}}{F_v}\right)^2 = \frac{25}{9} \qquad (21c)$$

For point 11

$$\frac{4(d-\bar{y}-t_f)^2}{d^2}\left(\frac{I_g}{I_n}\right)^2\left(\frac{f_{bg}}{F_b}\right)^2 + \frac{8}{3}\cdot\frac{V_B}{V}\cdot\frac{(d-\bar{y}-t_f)}{d}\cdot\frac{I_g}{I_n}\cdot\frac{(A_W)(a)(y_5)}{I_B}\cdot\frac{f_{vg}}{F_v}\cdot\frac{f_{bg}}{F_b}$$

$$+\left[\left(\frac{2A_W\, a\, y_5}{3I_B}\right)^2 + \frac{4}{3}\cdot\frac{d^2}{(d_B - t_f)^2}\right]\left(\frac{V_B}{V}\right)^2\left(\frac{f_{vg}}{F_v}\right)^2 = \frac{25}{9} \qquad (21d)$$

Governing Yield Curves

The critical stresses might occur at any of the twelve points shown in Fig. 3. To determine which of these points govern yielding, interaction curves with coordinates of f_{bg}/F_b and f_{vg}/F_v are constructed using the yield equations mentioned above. To construct these curves using the form of Eqs. (19) and (21) it is necessary to consider a specific beam and opening size. For points 1,3, 4,6,7,9,10,12, where the shearing stress is zero, the yield eqations, Eq. (19a) through Eq. (19h), are linear function of the coordinates. For points at the interface of the web and flange the yield equations, Eq. (21a) through Eq.(21d), are parabolic function of the coordinates.

As an example of the use of interaction curves to determine yielding, two beams are used as an illustrative design problem in Part III of this report. The beams considered are a W24 x 84 with a 19 in. wide by 12 in. deep opening

centered at mid-depth and a W30 x 108 with the same size of opening at a three-inch eccentricity. Of particular interest is the change in the capacity of the beams for differing amounts of reinforcement around the opening. The reinforcement considered here is added to the beam by welding straight rectangular bars of area A_r above and below the opening on one side of the web as shown in Fig. 4. To allow for the welds, the bars are placed 0.25 in. from the edges of the opening. By applying the yield equations to these two beams with varying amount of reinforcement around the opening the yield curves may be constructed. A different set of interaction curves is required for each different amount of reinforcing. Three interaction curves for reinforcement areas A_r of 0.0, 1.0 and 2.0 square inches are presented for each beam in Figs. 5, 6, 7, 8, 9, 10. Consideration of these yield curves shows that point 3 at the top edge of the opening, at the low moment section, and point 7 at the extreme fiber of the top T-section, at the high moment section, always govern yielding. The interaction curves of these two points construct a governing yield curve.

Design Curves

To obtain design formulas it is necessary to apply a safety factor to the yield stress to obtain allowable working stress. For points where $f_{vn}=0$, the yield equation of the form shown in Eq. (9) may be written as

$$\frac{f_{bn}}{F_b} = \frac{5}{3} \tag{22}$$

For design purposes f_{bn} must not be larger than the allowable bending stress F_b. Hence, a safty factor of 0.6 is applied to the sight side of Eq. (22) giving the design equation as

$$\frac{f_{bn}}{F_b} = 1 \tag{23}$$

The design equations for points 1, 3, 4, 6, 7, 9, 10, 12 are obtained by multiplying a safety factor of 0.6 to the right side of the yield equations stated as Eq. (19a) through Eq. (19h). For example, the design equation for point 3 is

$$\frac{2(\bar{y} - d_T)}{d} \cdot \frac{I_g}{I_n} \cdot \frac{f_{bg}}{F_b} + \frac{2}{3} \cdot \frac{V_T}{V} \cdot \frac{(A_W)(a)(y_3)}{I_T} \cdot \frac{f_{vg}}{F_v} = 1 \qquad (24)$$

and for point 7

$$\frac{2\bar{y}}{d} \cdot \frac{I_g}{I_n} \cdot \frac{f_{bg}}{F_b} + \frac{2}{3} \cdot \frac{V_T}{V} \cdot \frac{(A_W)(a)(y_1)}{I_T} \cdot \frac{f_{vg}}{F_v} = 1 \qquad (25)$$

Since points 3 and 7 govern yielding, the design curves are obtained by plotting these two equations. The design curves for a W24 x 84 with a 19" x 12" concentric opening and a W30 x 108 with the same size of opening but with 3" eccentricity are shown in Fig. 11 and Fig. 12, for varying amounts of reinforcement.

Application of Design Curves

In design of a beam with a web opening, a section is selected by the usual approach for designing a beam without a web opening. Then the internal beam force curve is drawn for the selected section for the given loading condition and it is compared with the design curves of this section with various amounts of reinforcement. If the internal beam force curve falls below a design curve, it is a safe design with that amount of reinforcement. If the internal beam force curve falls above the design curve, that amount of reinforcement is not adequate, and the amount of reinforcement should be increased. When the internal beam force curve intersects the design curve, the opening is allowed only for a part of the beam.

To draw the internal beam force curve the equations for shearing force and

bending moment are written in term of the distance from the support x, then f_{bg}/F_b and f_{vg}/F_v are calculated. The internal beam force equation is obtained by eliminating x from these two equations. The application of the design curves is illustrated in the following example.

PART III : DESIGN EXAMPLE

PROBLEM STATEMENT

A portion of the floor system supporting a concourse in a multi-story building is shown in Fig. 13. The floor system consists of a girder spanning from column to column with floor beams supported by the girders. The floor beams and girders support a 4-inch concrete slab which in turn provides continuous lateral support to the top flanges of the floor members. Moment connections are provided between the columns and the girders, and therefore the girder ends are assumed to be fixed. It is further assumed that the columns are W14 sections and the girder span is taken from column face to column face. The floor beams are attached to the girders with shear connections and simple supports are therefore assumed.

The heating, ventilation, and air conditioning (HVAC) ducts run parallel to the girders with service ducts branching out at right angles. For both architectural and esthetic reasons it is undesirable to run the HVAC system below the floor members, so they must penetrate them. It is also desirable to keep the HVAC system on a level plane, thereby reducing installation costs by decreasing the number of bends in the duct material. It is necessary to provide a duct area of 144 square inches with 1-inch thick insulation on all sides. Vertical positioning of the ducts used in this example are shown in Fig. 14.

The floor system is to be designed to carry a live load of 100 psf (from Uniform Building Code) and a dead load of 80 psf (50 psf for the concrete slab and 30 psf for other dead load). Using A36 steel and the AISC Specification for elastic design along with the design curves developed, the locations where openings can be placed along the length of the floor beams and girders will be explored with varying amounts of opening reinforcement.

Data for this example has been taken from Reference (9).

FLOOR BEAMS

Selection of Beam Section

The loading condition is shown in Fig. 15

Uniformly Distributed Load: $w = (0.10 + 0.08) \times 12 = 2.16$ kips/ft.

Design Moment: $M = (2.16)(35)^2/8 = 330.75$ kips-ft.

Allowable Bending Stress $F_b = 0.6\ F_y$ (AISC)

For A36 Steel: $F_b = (0.6)(36) = 21.6$ ksi

Required Section Modulus: $S = (330.75)(12)/21.6 = 184$ in.^{3}

Try W24 x 84 ($S = 197$ in.$^3 > 184$ in.^{3})

For W24 x 84 $I = 2370$ in.^{4} $d = 24.09$ in. $t_w = 0.47$ in.

Allowable Shearing Stress $F_v = 0.4\ F_y$ (AISC)

For A36 Steel: $F_v = (0.4)(36) = 14.4$ ksi

Design Shear: $V = (2.16)(35)/2 = 37.8$ kips

Allowable Shear: $V = (14.4)(0.47)(24.09) = 163$ kips > 37.8 kips

Use W24 x 84

Opening Parameters

Depth of opening: $H = 12$ in. Width of opening: $2a = 19$ in.

Eccentricity: $e = 0$

Calculation of Internal Beam Force Equation

The shear and moment along the beam are obtained from the shear and moment diagrams shown in Fig. 16 and Fig. 17.

$$f_{vg} = \frac{V}{A_W} = \frac{37.8 - 2.16x}{(24.09)(0.470)} = \frac{37.8 - 2.16x}{11.32}$$

$$\frac{f_{vg}}{F_v} = \frac{(37.8 - 2.16x)/11.32}{14.4} = \frac{37.8 - 2.16x}{163} \qquad (26)$$

$$f_{bg} = \frac{Mc}{I} = \frac{(37.8x - 1.08x^2)(12)(24.09/2)}{2370} = \frac{37.8x - 1.08x^2}{16.4}$$

$$\frac{f_{bg}}{F_b} = \frac{(37.8x - 1.08x^2)/16.4}{21.6} = \frac{37.8x - 1.08x^2}{354.24} \qquad (27)$$

By solving Eq. (26) for x and substituting into Eq. (27) the internal beam force equation is obtained as

$$\frac{f_{bg}}{F_b} = 0.934 - 17.36\left(\frac{f_{vg}}{F_v}\right)^2 \qquad (28)$$

Location of the Opening

The method used to determine where an opening may be positioned along the beam is explained in this section. A plot of the internal beam force curve as given by Eq. (28) is superimposed on the design curves for the W24 x 84 floor beam as shown in Fig. 11. By substituting into Eq. (27) the value of f_{bg}/F_b for points where these two curves intersect, the minimum distance x from the support at which the opening may be positioned is found. By taking A_r = 0.5 sq. in. as an example, the value of f_{bg}/F_b at the intersection point found from Fig. 11 is 0.635. Substituting this value into Eq. (27) gives x = 7.6 ft. Hence the opening must be placed at least 7.6 ft. from the supports. The permissible opening locations with varying amounts of reinforcement are shown in Fig. 18.

GIRDER

The loading condition of the girder is shown in Fig. 19. The shear and moment diagrams due to the load are shown in Fig. 20 and Fig. 21. The AISC Specification allows a reduction of the maximum negative moment of one-tenth if the maximum positive moment is increased by one-tenth of the average negative moment. From the moment diagram shown in Fig. 19, the moment at the ends become 522 kips-ft. with the nine-tenth rule applied, and the moments at the loading points increases to 340 kips-ft. as shown in Fig. 22.

Selection of Section

Load $P = 2.16 \times 35 = 75.6$ kips

Design Moment $M = 522$ kips-ft.

Allowable Bending Stress $F_b = 0.6\ F_y$ (AISC)

For A36 Steel $F_b = 21.6$ ksi

Required Section Modulus $S = (522)(12)/21.6 = 290$ in.^{3}

Try W30 x 108 ($S = 300$ in.$^3 > 290$ in.^{3})

For W30 x 108 $d = 9.82$ in. $I = 4470$ in.^{4} $t_w = 0.548$ in.

Allowable Shearing Stress $F_v = 0.4\ F_y$ (AISC)

For A36 Steel $F_v = 14.4$ ksi

Design Shear Force $V = 75.6^k$

Allowable Shear Force $V = (14.4)(29.82)(0.548) = 235^k > 75.6^k$

Use W30 x 108

Opening Parameters

Depth of opening $H = 12$ in. Width of opening $2a = 19$ in.

Eccentricity of opening $e = 29.82/2 - 24.09/2 = 2.87$ in.

Use $e = 3$ in.

Calculation of Internal Beam Force Equation

Two regions must be investigated since the shears are different. For the region between the loads, the shear force is zero, and the moment is a constant, hence

$$\frac{f_{vg}}{F_v} = 0$$

and

$$\frac{f_{bg}}{F_b} = \frac{(282)(12)(29.82/2)}{4470 \times 21.6} = 0.630$$

The internal beam force curve is only a point for this region.

For regions between ends and loads

$$f_{vg} = \frac{V}{A_W} = \frac{75.6}{0.548 \times 29.82} = 4.626$$

$$\frac{f_{vg}}{F_v} = \frac{4.626}{14.4} = 0.321 \qquad (29)$$

$$f_{bg} = \frac{Mc}{I} = \frac{(-579.5 + 75.6x)(12)(29.82/2)}{4470} = \frac{(-579.5 + 75.6x)}{24.98}$$

$$\frac{f_{bg}}{F_b} = \frac{(-579.5 + 75.6x)/24.98}{21.6} = \frac{-579.5 + 75.6x}{540} \qquad (30)$$

Since f_{vg}/F_v is a constant, f_{bg}/F_b is a vertical line on the internal beam force curve and has a maximum value at $x = 0$ of 1.07.

Location of the Opening

The plot of the internal beam force curve as given by Eq. (30) is superimposed on the design curves for the W30 x 108 girder as shown in Fig. 12. By substituting into Eq. (30) the value of f_{bg}/F_b for points where the two curves intersect, the maximum distance x from the support at which the opening may be placed is found. By taking A_r = 1.0 sq. in. as an example, the value of f_{bg}/F_b at the intersection point found from Fig. 12 is 0.140. Substituting this value into Eq. (30) gives x =8.66'. Further restrictions are placed on opening locations in girders in the vincinity of concentrated loads and reactions. It is recommended in Reference (1) that the edge of the opening be a distance of at least d/2 from the points where concentrated loads or reactions are introduced unless stiffeners are provided. Hence the opening may be placed in the region of 15 in. from the supports to 8.66' from the supports. The permissible opening locations for girder with varying amounts of reinforcement are shown in Fig. 23.

CONCLUSIONS

A comparison of experimental results from tests on full size steel beams to theoretical stresses found using the Vierendeel method shows good agreement at critical points. Hence, the Vierendeel method is assumed to be sufficiently accurate for design purposes.

Consideration of the yield curves for points of high stress, which were obtained using the von Mises yield theory, shows two points to be critical for the amount of opening reinforcement studied. These points are at the upper edge of the opening at the low moment section and the top extreme fiber at the high moment section, when the eccentricity of the opening is above mid-depth.

The use of design curves to determine the amount of reinforcement required for a certain size of opening and the locations along the beam where the opening may be placed, was found to be an effective approach.

RECOMMENDATIONS FOR FURTHER RESEARCH

In this report concentric and eccentric web opening with reinforcement were studied. The maximum amount of reinforcement used was 2.0 sq. in., and only rectangular openings were considered. For further investigation of beams with web openings, the following items are suggested :

(1) Investigate additional sizes of beams and openings, and types of loading.

(2) Investigate which of the points of high stress are critical for opening reinforcements exceeding A_r=2.0 sq. in..

(3) Study the economy of using eccentric openings by investigating differences in the amount of reinforcement required for concentric and eccentric openings of the same size.

ACKNOWLEDGEMENTS

The author wishes to express sincere appreciation to Dr. Harry D. Knostman for serving as major professor. Without his ready assistance and able guidance this report would not have been possible. The author also wishes to thank Dr. Peter B. Cooper for correcting many grammatical mistakes to make this report more readible.

APPENDIX I - REFERENCES

1. "Suggested Design Guide for Beams with Web Holes," Journal of Structural Division, ASCE, Vol. 97, No. ST11, Proc. Paper 8536, November, 1971, pp. 2707-2728.
2. Redwood, R. G. and Peter W. Chan, "Design Aid for Beams with Circular Eccentric Web Holes," Journal of Structural Division, ASCE, Vol. 100, No. ST2, Proc. Paper 10331, February, 1974, pp. 297-302.
3. Bower, J. E., "Design of Beams with Web Openings," Journal of Structural Division, ASCE, Vol. 94, No. ST3, Proc. Paper 5869, March, 1968, pp. 783-807.
4. Douglas, T. R. and S. C. Gambrell, Jr., "Design of Beams with Off-center Web Openings," Journal of Structural Division, ASCE, Vol. 100, No. ST6, Proc. Paper 10611, June, 1974, pp. 1189-1203.
5. Wang, T. M., R. R. Snell and P. B. Cooper, "Strength of Beams with Eccentric Reinforced Holes," Journal of Structural Division, ASCE, Vol. ST9, Proc. Paper 11540, September, 1975, pp. 1783-1800.
6. Ahmad, S. H., "Elastic Tests of Steel Beams with Reinforced Eccentric Web Opening," Master's Thesis, Department of Civil Engineering, Kansas State University, August, 1975.
7. Cowper, G. R., "The Shear Coefficient in Timoshenko's Beam Theory," Transaction, ASME, Series E, Vol. 33, June, 1966, pp. 334-340.
8. Frost, R. W., "Behavior of Steel Beams with Eccentric Web Holes," Technical Report 46.019-400(1), Research Laboratory, United States Steel Corporation, February, 1973.
9. Kussman, R. L., "Beams with Web Openings : Ultimate Load Tests and Design Example," Master's Thesis, Department of Civil Engineering, Kansas State University, 1975.

APPENDIX II - NOTATION

The following symbols are used in this report :

A = Coefficient - f_{bn}/f_{bg} ;

A_f = Area of one flange - $b_f \cdot t_f$;

A_r = Area of reinforcement above opening, also area of reinforcement below opening - $b_r \cdot t_r$;

A_W = Web area - $d\ t_w$;

A_{WB} = Web area of bottom T-section - $(d_B - t_f)\ t_w$;

A_{WT} = Web area of top T-section - $(d_T - t_f)\ t_w$;

B = Coefficient - f_{vn}/f_{vg} ;

E = Modulus of elasticity ;

F_b = Allowable bending stress - $0.6\ F_y$;

F_v = Allowable shearing stress - $0.4\ F_y$;

F_y = Yield stress of steel ;

G = Shear Modulus ;

H = Depth of the opening ;

HMS = High moment section ;

I_B = Moment of inertia of bottom section ;

I_g = Moment of inertia of gross section ;

I_n = Moment of inertia of net section ;

I_T = Moment of inertia of top section ;

K = Shear deflection coefficient ;

LMS = Low moment section ;

M_o = Primary bending moment at vertical centerline of opening ;

M = Bending moment ;

M/V = Moment to shear ratio ;

N. A. = Neutral axis ;

P = Load ;

S = Section modulus ;

V = Shear force ;

V_B = Shear force in bottom section ;

V_T = Shear force in top section ;

V_T/V_B = Shear distribution ratio ;

a = Half-width of opening ;

b_f = Width of flange ;

c = Width of reinforcement ;

d = Depth of the beam ;

d_B = Depth of bottom T-section ;

d_T = Depth of top T-section ;

e = Eccentricity - distance between mid-depth of beam and mid-depth of opening ;

f_B = Normal stress in bottom section ;

f_{bg} = Bending stress in gross section ;

f_{bn} = Bending stress in net section ;

f_{vg} = Shearing stress in gross section ;

f_{vn} = Shearing stress in net section ;

f_T = Normal stress in top section ;

q = Thickness of reinforcement ;

t_f = Flange thickness ;

t_w = Web thickness ;

u = Distance from the edge of opening to nearest edge of reinforcement ;

x_o = Longitudinal distance from vertical centerline of the opening ;

y_B = Distance from the neutral axis of the bottom section to any fiber in the section, measured positive down ;

y_n = Distance from the neutral axis of the net section to any fiber, measured positive down ;

y_T = Distance from the neutral axis of the top section to any fiber in the section, measured positive down ;

y_1 = Distance from the neutral axis of the top section to the extreme top fiber, measured positive down ;

y_2 = Distance from the neutral axis of the top section to the interface of the web and flange in the top section, measured positive down ;

y_3 = Distance from the neutral axis of the top section to the top edge of the opening, measured positive down ;

y_4 = Distance from the neutral axis of the bottom section to the bottom edge of the opening, measured positive down ;

y_5 = Distance from the neutral axis of the bottom section to the interface of the web and flange, measured positive down ;

y_6 = Distance from the neutral axis of the bottom section to the extreme bottom fiber, measured positive down ;

$\bar{y}$ = Distance from the neutral axis of the net section to the extreme top fiber, measured positive down.

Table 1. Dimensions of Beams Tested at Kansas State University (in inches).

Beam	Size	2a	H	d	d_T	d_B	b_f	t_f	t_w	c	q	u
1	W16 x 45	9.0	6.04	16.11	3.14	6.93	7.00	0.539	0.374	0.374	-----	-----
2	W16 x 45	9.0	6.01	16.11	3.02	7.08	6.99	0.539	0.380	2.350	0.241	0.27
3	W16 x 40	12.0	6.09	16.10	3.01	7.00	7.03	0.475	0.334	0.334	-----	-----
4	W16 x 40	12.0	6.09	16.10	3.01	7.00	7.03	0.475	0.334	2.334	0.250	0.25
5	W16 x 40	12.0	6.09	16.10	3.01	7.00	7.03	0.475	0.334	4.334	0.250	0.25
5a	W16 x 40	12.0	6.09	16.10	7.00	3.01	7.03	0.475	0.334	4.334	0.250	0.25

Table 2. Comparison of Experimental and Theoretical Values of f/V for Test Beam 1.

LEVEL	M/V	HIGH MOMENT SECTION			LOW MOMENT SECTION		
		Experimental f/V in.$^{-2}$	Theoretical f/V in.$^{-2}$	Difference %	Experimental f/V in.$^{-2}$	Theoretical f/V in.$^{-2}$	Difference %
1	20	-0.485	-0.456	5.98	-0.095	-0.162	-70.52
	40	-0.776	-0.765	1.42	-0.385	-0.471	-22.34
	60	-1.063	-1.074	-1.03	-0.675	-0.780	-15.55
	80	-1.356	-1.383	-1.99	-0.968	-1.089	-12.50
2	20	0.524	0.439	8.50	-1.000	-0.827	17.3
	40	0.234	0.245	-4.70	-1.258	-1.021	18.84
	60	-0.036	0.050	-----	-1.530	-1.215	20.59
	80	-0.323	-0.143	55.73	-1.800	-1.409	21.72
3	20	-0.631	-0.461	26.94	0.642	0.515	19.78
	40	-0.592	-0.434	26.69	0.663	0.542	18.25
	60	-0.607	-0.408	32.78	0.681	0.568	16.59
	80	-0.601	-0.381	36.60	0.693	0.595	14.14
4	20	0.432	0.428	0.93	0.139	0.132	5.03
	40	0.705	0.709	-0.57	0.420	0.412	1.94
	60	0.995	0.989	0.60	0.699	0.693	0.86
	80	1.276	1.269	0.55	0.989	0.973	1.62

Table 3. Comparison of Experimental and Theoretical Values of f/V for Test Beam 2.

LEVEL	M/V	HIGH MOMENT SECTION			LOW MOMENT SECTION		
		Experimental f/V in.$^{-2}$	Theoretical f/V in.$^{-2}$	Difference %	Experimental f/V in.$^{-2}$	Theoretical f/V in.$^{-2}$	Difference %
1	20	-0.453	-0.429	5.30	-0.118	-0.120	-1.69
	40	-0.731	-0.704	3.70	-0.400	-0.394	1.50
	60	-1.027	-0.978	4.77	-0.687	-0.668	2.77
	80	-1.311	-1.252	4.50	-0.980	-0.943	3.78
2	20	0.337	0.536	59.05	-0.855	-0.888	-3.86
	40	0.086	0.360	-----	-1.089	-1.065	2.20
	60	-0.172	0.183	-----	-1.338	-1.241	7.25
	80	-0.423	0.007	-----	-1.578	-1.417	10.20
3	20	-0.453	-0.428	5.52	0.450	0.466	-3.55
	40	-0.456	-0.408	10.53	0.459	0.485	-5.66
	60	-0.456	-0.389	14.69	0.465	0.505	-8.60
	80	-0.444	-0.370	16.67	0.483	0.524	-8.49
4	20	0.409	0.376	8.07	0.148	0.123	16.89
	40	0.666	0.625	6.16	0.403	0.373	7.44
	60	0.947	0.875	7.60	0.684	0.622	9.06
	80	1.234	1.124	8.91	0.974	0.872	10.47

Table 4. Comparison of Experimental and Theoretical Values of f/V for Test Beam 3.

LEVEL	M/V	HIGH MOMENT SECTION			LOW MOMENT SECTION		
		Experimental f/V in.$^{-2}$	Theoretical f/V in.$^{-2}$	Difference %	Experimental f/V in.$^{-2}$	Theoretical f/V in.$^{-2}$	Difference %
1	20	-0.585	-0.537	8.20	-0.079	-0.146	-84.81
	40	-0.917	-0.894	2.51	-0.425	-0.493	-16.00
	60	-1.250	-1.241	0.72	-0.765	-0.840	-9.80
2	20	0.743	0.690	7.13	-1.408	-1.137	19.25
	40	0.425	0.467	-9.88	-1.687	-1.361	19.32
	60	0.124	0.243	-95.96	-1.969	-1.584	19.55
3	20	-1.070	-0.815	23.83	0.991	0.867	12.51
	40	-1.101	-0.789	28.33	0.969	0.893	7.84
	60	-1.076	-0.763	29.09	0.990	0.918	7.27
4	20	0.532	0.566	-6.39	0.070	0.059	15.71
	40	0.796	0.878	-10.30	0.340	0.371	-9.12
	60	1.129	1.191	-5.49	0.685	0.684	0.15

Table 5. Comparison of Experimental and Theoretical Values of f/V for Test Beam 4.

LEVEL	M/V	HIGH MOMENT SECTION			LOW MOMENT SECTION		
		Experimental f/V $in.^{-2}$	Theoretical f/V $in.^{-2}$	Difference %	Experimental f/V $in.^{-2}$	Theoretical f/V $in.^{-2}$	Difference %
1	20	-0.554	-0.506	8.66	-0.079	-0.146	-84.81
	40	-0.869	-0.832	4.26	-0.408	-0.472	-15.69
	60	-1.196	-1.159	3.09	-0.735	-0.798	-8.57
2	20	0.526	0.321	38.97	-1.070	-0.735	31.30
	40	0.247	0.114	53.85	-1.326	-0.942	28.96
	60	-0.028	-0.093	———	-1.582	-1.150	27.31
3	20	-0.833	-0.464	44.30	0.766	0.532	30.55
	40	-0.825	-0.431	47.76	0.790	0.566	28.35
	60	-0.822	-0.397	51.70	0.810	0.600	25.93
4	20	0.500	0.515	-3.00	0.070	0.106	-51.43
	40	0.785	0.826	-5.22	0.363	0.415	-14.33
	60	1.083	1.137	-4.99	0.654	0.728	-11.31

Table 6. Comparison of Experimental and Theoretical Values of f/V for Test Beam 5.

LEVEL	M/V	HIGH MOMENT SECTION			LOW MOMENT SECTION		
		Experimental f/V $in.^{-2}$	Theoretical f/V $in.^{-2}$	Difference %	Experimental f/V $in.^{-2}$	Theoretical f/V $in.^{-2}$	Difference %
1	20	-0.511	-0.481	5.87	-0.082	-0.137	-67.07
	40	-0.807	-0.790	2.11	-0.394	-0.446	-13.20
	60	-1.122	-1.098	2.14	-0.698	-0.755	-8.17
2	20	0.227	0.181	20.26	-0.680	-0.568	16.47
	40	0.022	-0.012	-----	-0.861	-0.762	11.50
	60	-0.173	-0.206	19.07	-1.060	-0.955	9.91
3	20	-0.399	-0.316	20.82	0.370	0.396	-7.03
	40	-0.395	-0.276	30.13	0.385	0.436	-13.24
	60	-0.373	-0.236	36.73	0.394	0.476	-20.81
4	20	0.470	0.493	-4.89	-0.091	0.124	------
	40	0.742	0.801	-7.95	0.363	0.433	-19.28
	60	1.063	1.110	-4.42	0.681	0.741	-8.81

Table 7. Comparison of Experimental and Theoretical Values of f/V for Test Beam 5a.

LEVEL	M/V	HIGH MOMENT SECTION			LOW MOMENT SECTION		
		Experimental f/V in.$^{-2}$	Theoretical f/V in.$^{-2}$	Difference %	Experimental f/V in.$^{-2}$	Theoretical f/V in.$^{-2}$	Difference %
1	20	-0.483	-0.493	-2.07	-0.105	-0.124	-18.09
	40	-0.783	-0.801	-2.30	-0.412	-0.433	-5.10
	60	-1.081	-1.110	-2.68	-0.709	-0.741	-4.51
2	20	0.342	0.316	7.60	-0.424	-0.396	6.60
	40	0.321	0.276	14.02	-0.443	-0.436	1.58
	60	0.311	0.236	24.12	-0.449	-0.476	-6.01
3	20	-0.261	-0.181	30.65	0.653	0.568	13.02
	40	-0.081	0.012	-----	0.821	0.762	7.19
	60	0.119	0.206	-73.10	1.017	0.955	6.10
4	20	0.523	0.481	8.03	0.094	0.137	-45.74
	40	0.791	0.790	0.13	0.357	0.446	-24.93
	60	1.096	1.099	-0.27	0.664	0.755	-13.70

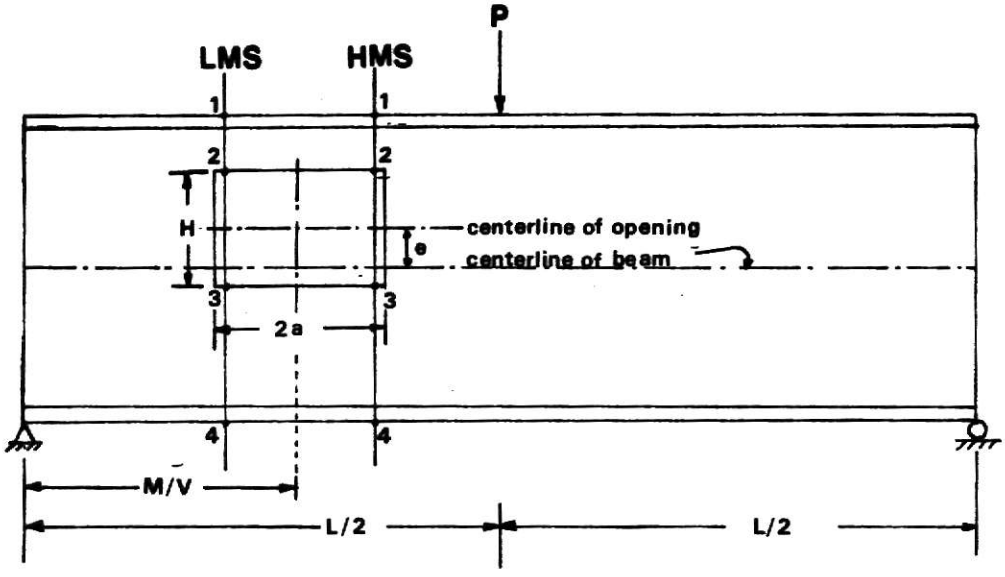

Fig. 1 Points Where Experimental Stresses are Compared to Vierendeel Stresses.

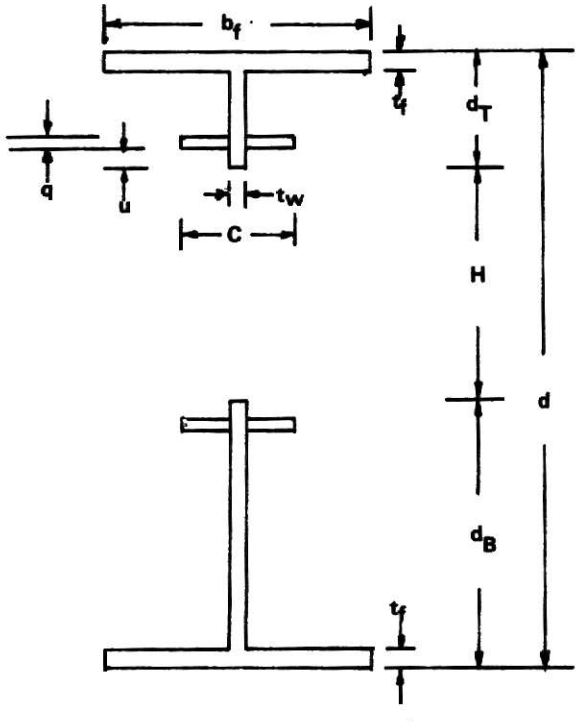

Fig. 2 General Cross-section of Test Beams.

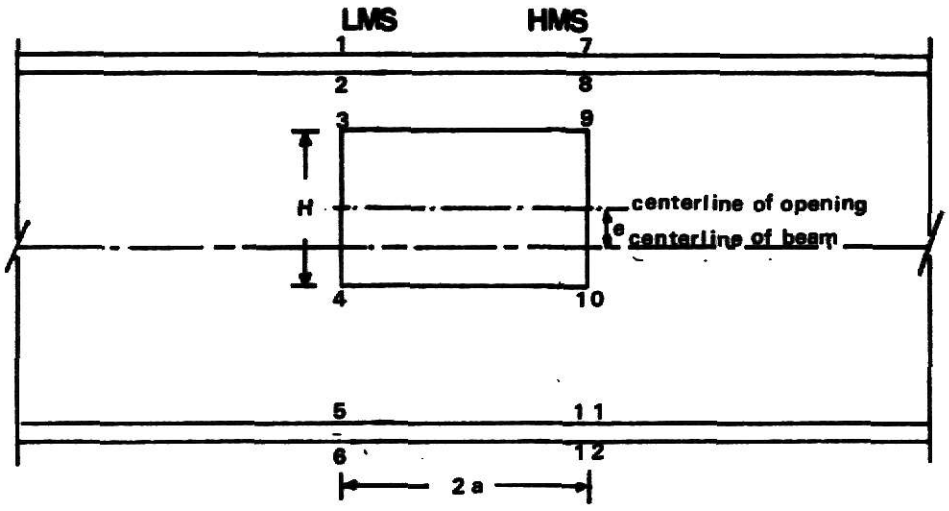

Figure 3 Twelve Investigated Points for Critical Stress.

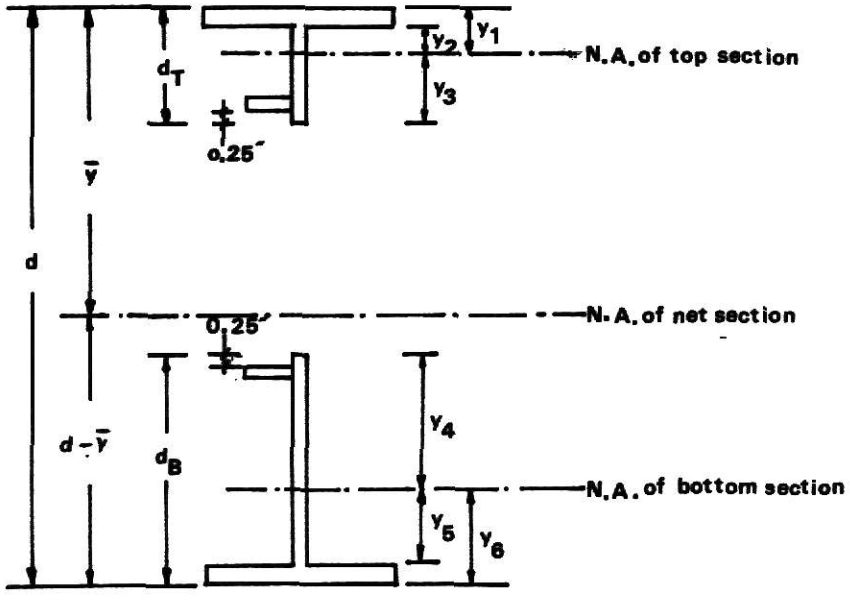

Figure 4 Cross-section at the Opening.

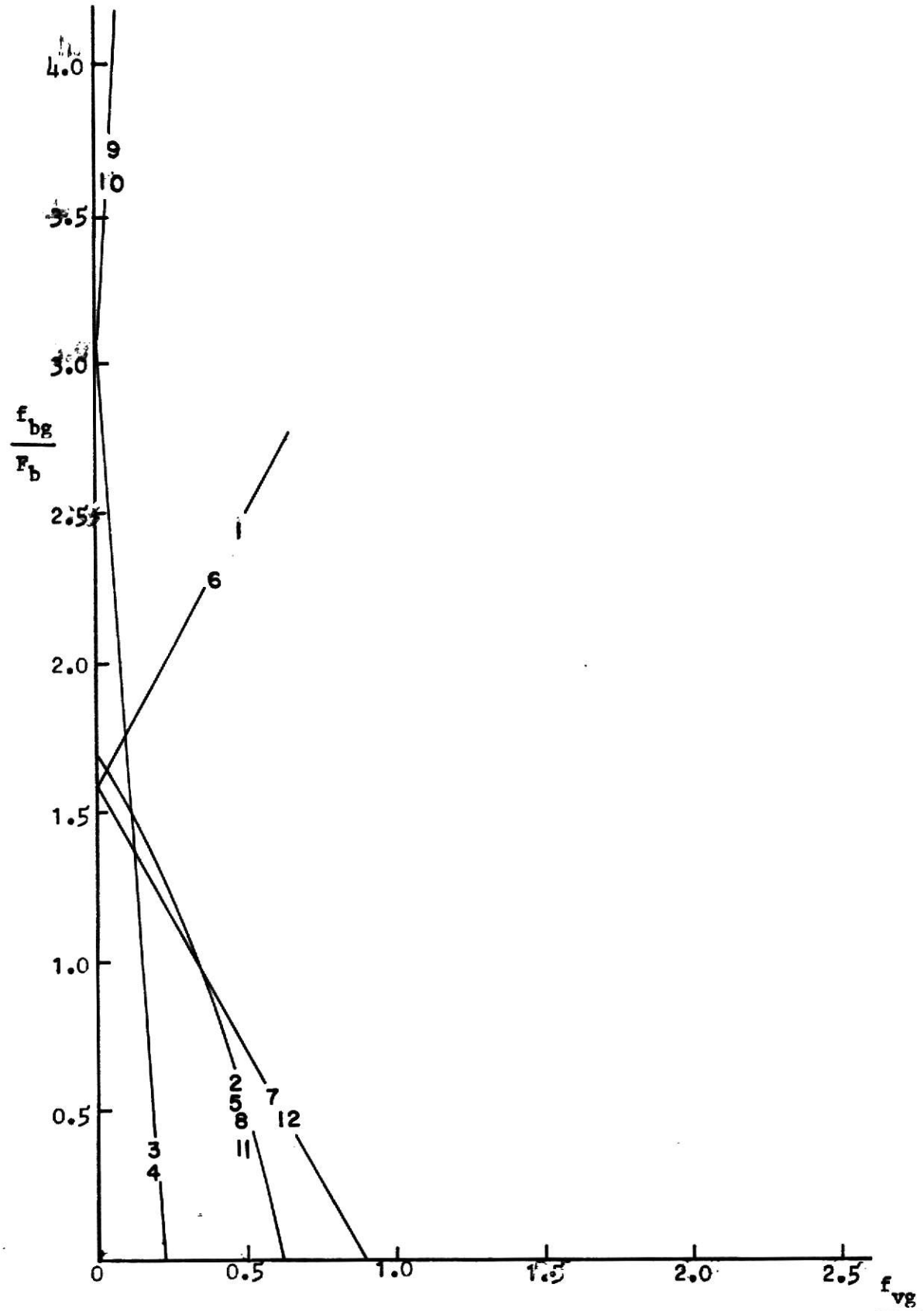

Figure 5 Yield Curves for W24 x 84 with A_r= 0, e=0.

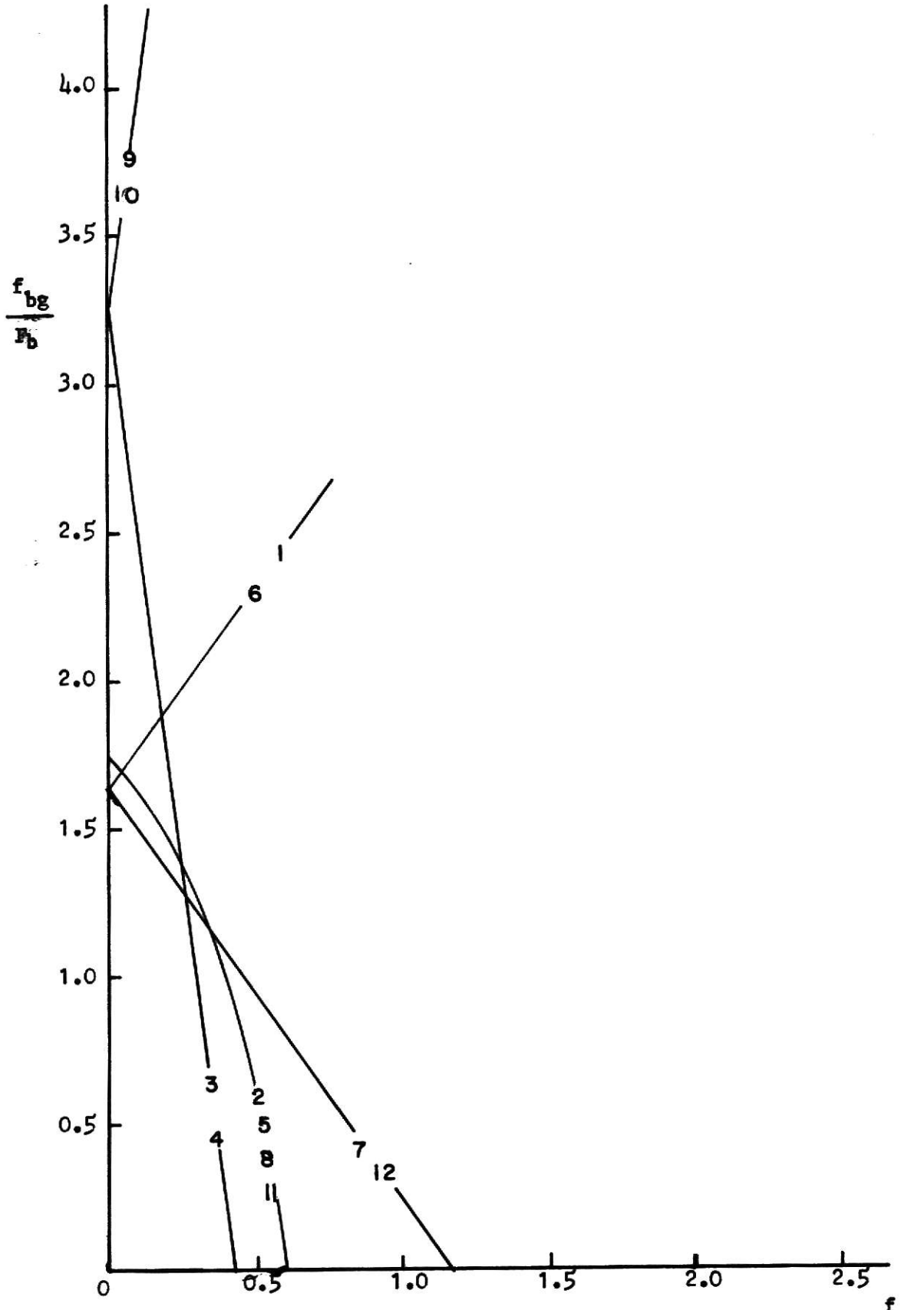

Figure 6 Yield Curves for W24 x 84 with A_r=1.0 sq.in., e=0.

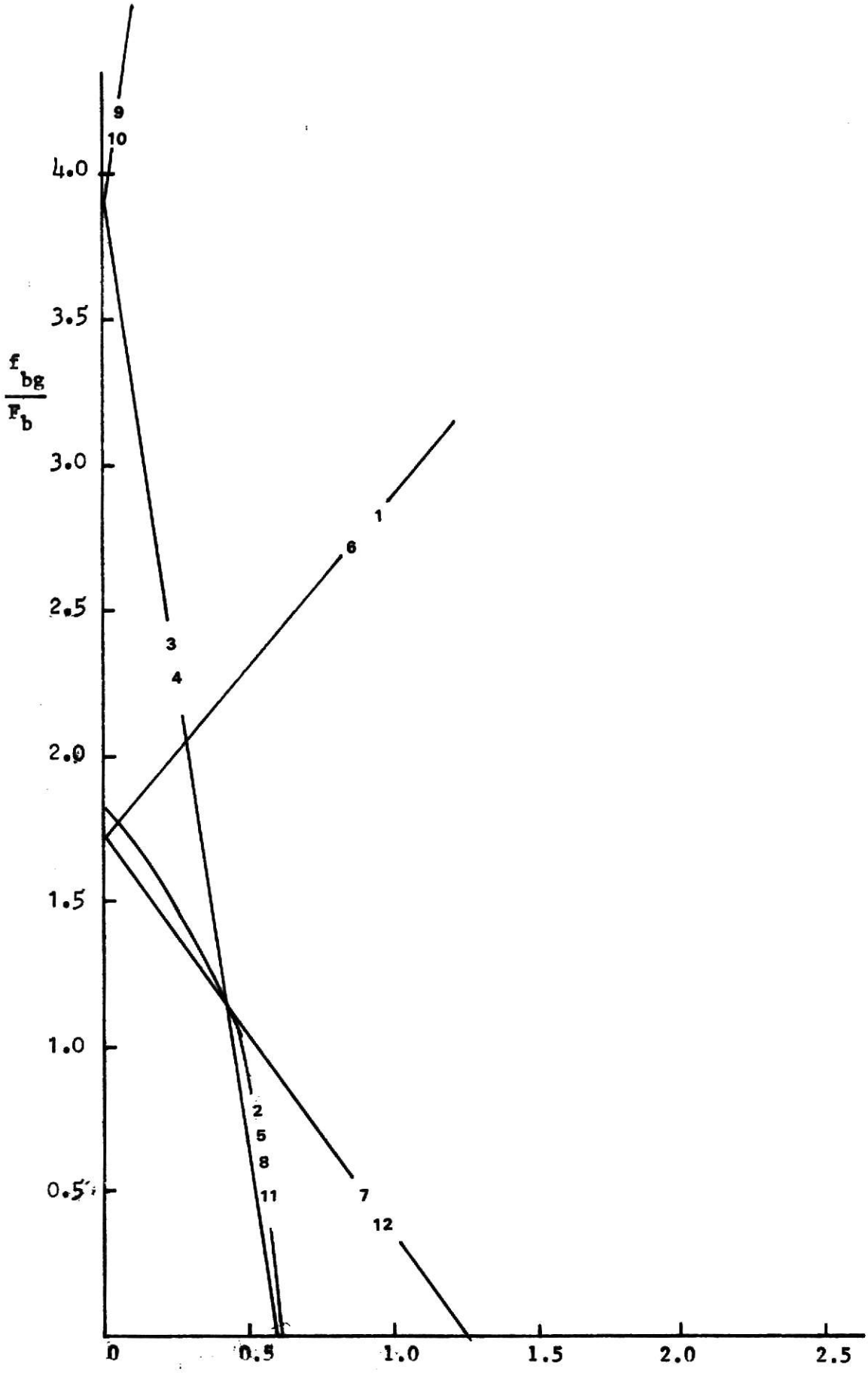

Figure 7. Yield Curves for W24 x 84 with A_T=2.0sq. in., e=0.

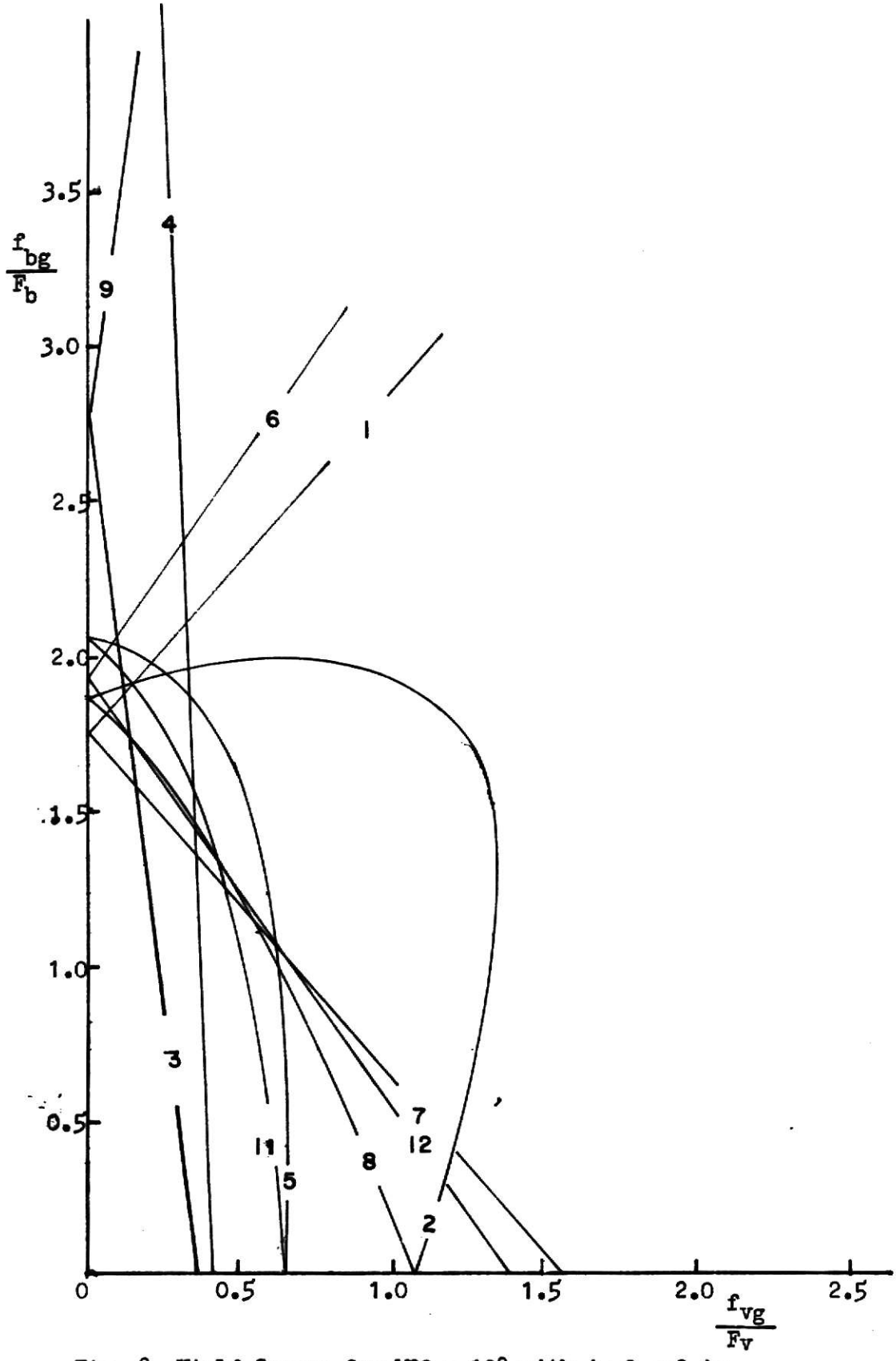

Fig. 8. Yield Curves for W30 x 108 with A_r=0, e=3 in.

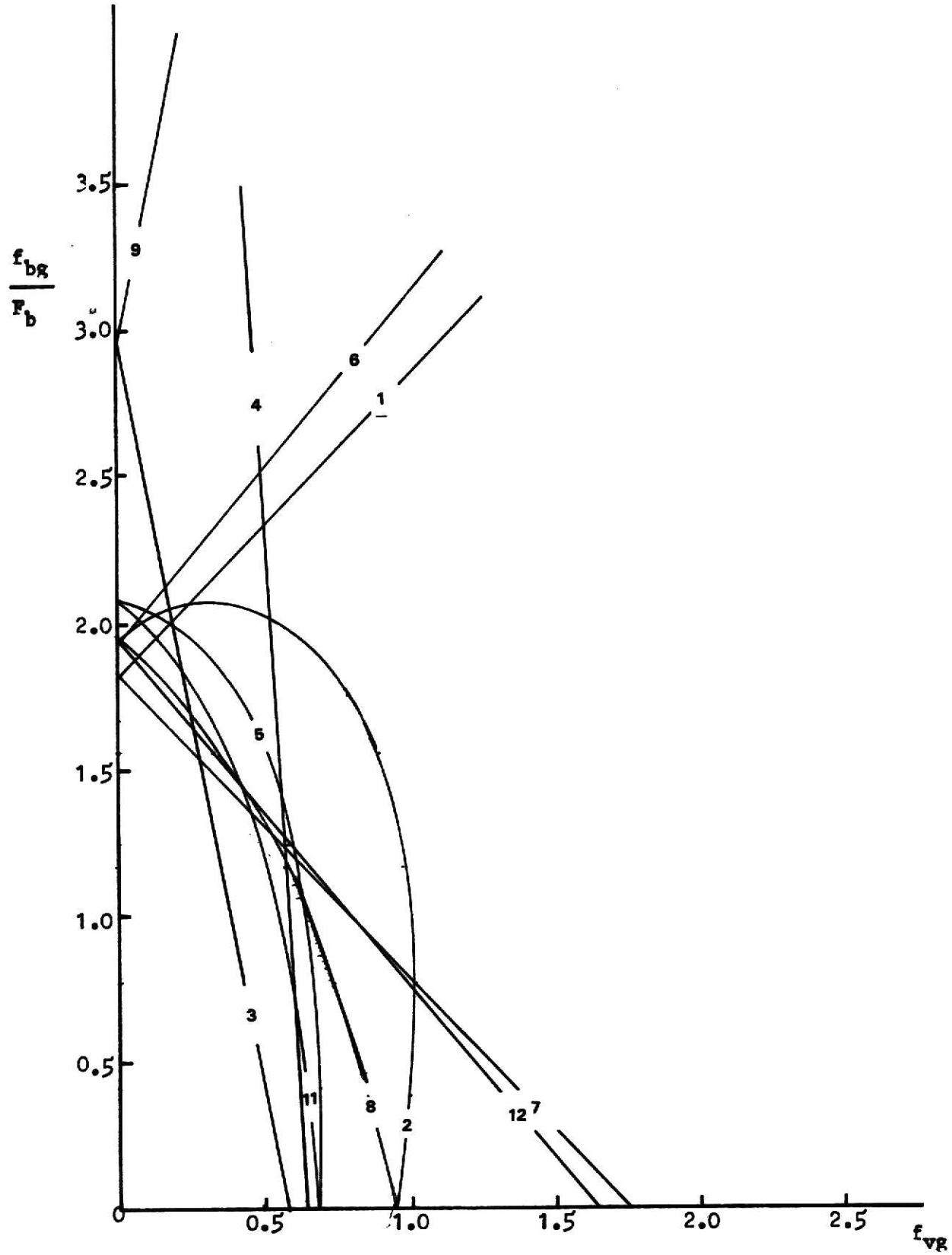

Figure 9. Yield Curves for W30x108 with A_T=1.0 sq. in., e=3 in.

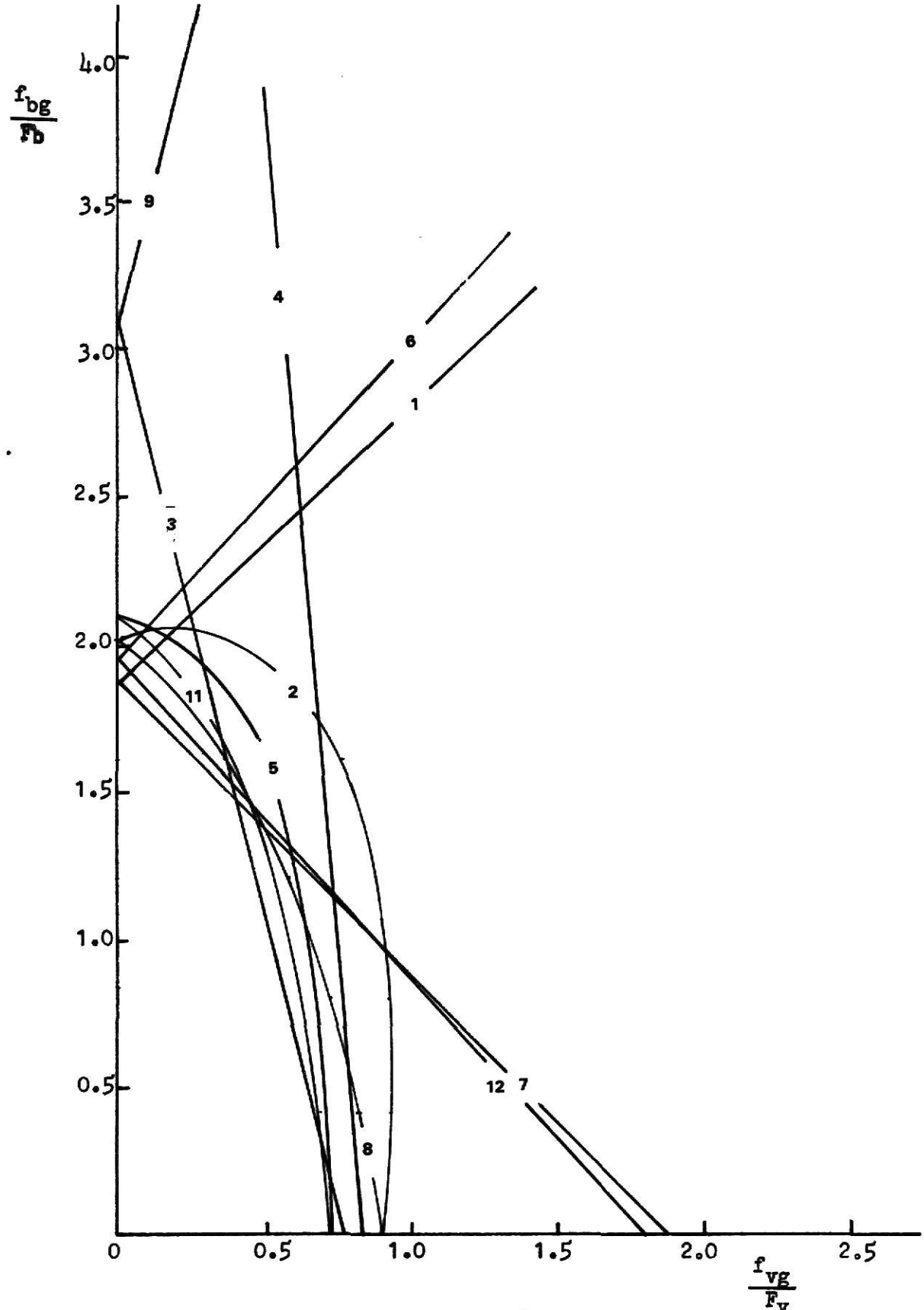

Fig. 10. Yield Curves for W30 x 108 with A_r=2.0 sq. in., e=3 in.

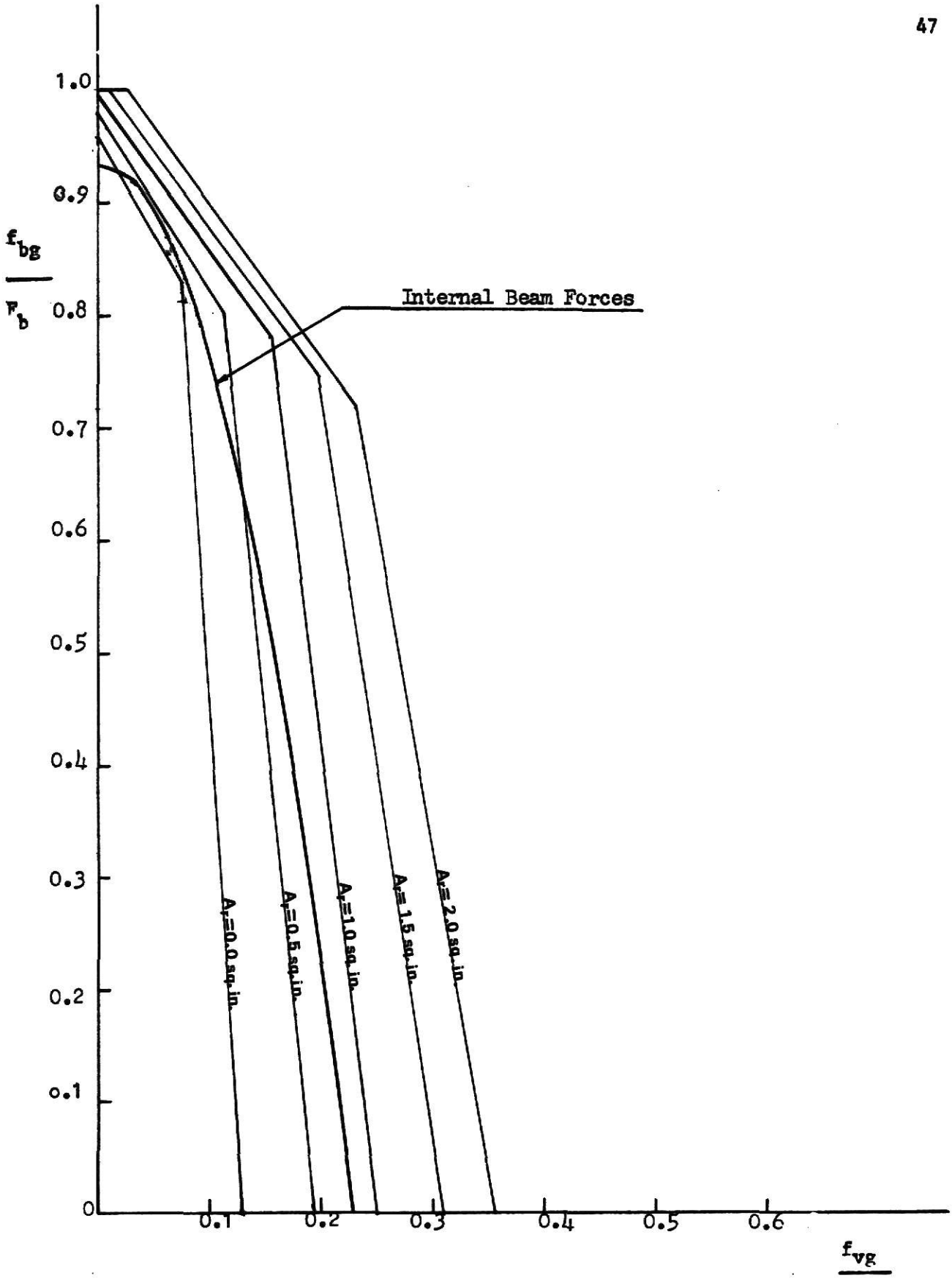

Figure 11. W24 x84 Floor Beam Design Curves.

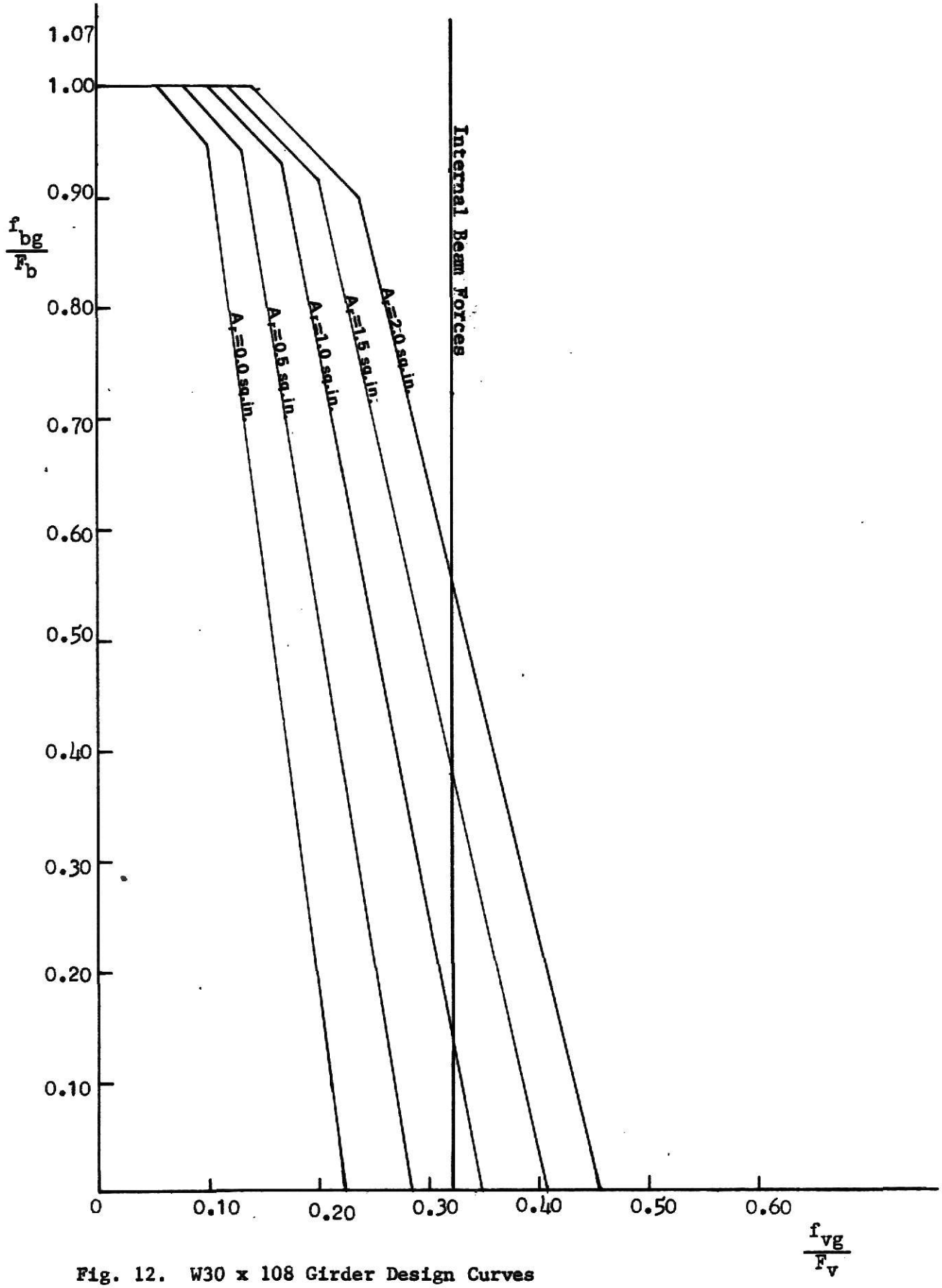

Fig. 12. W30 x 108 Girder Design Curves

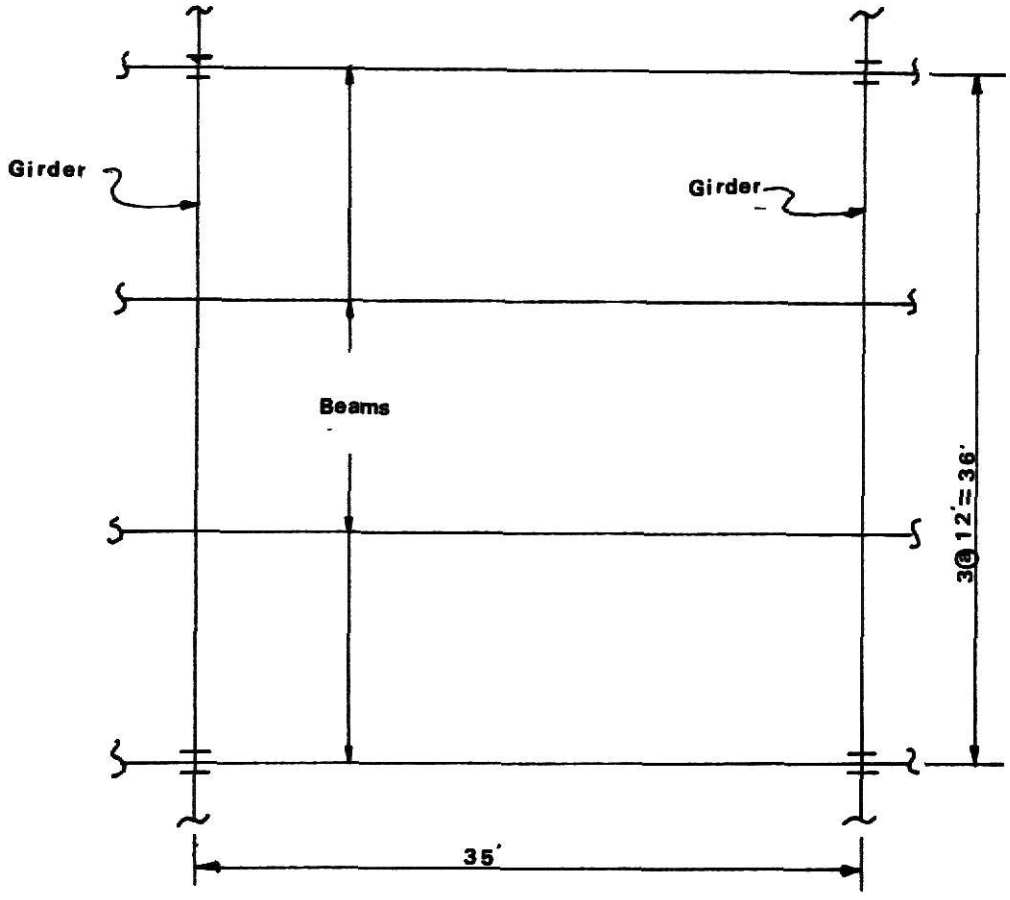

Fig. 13. Plan View of Floor System

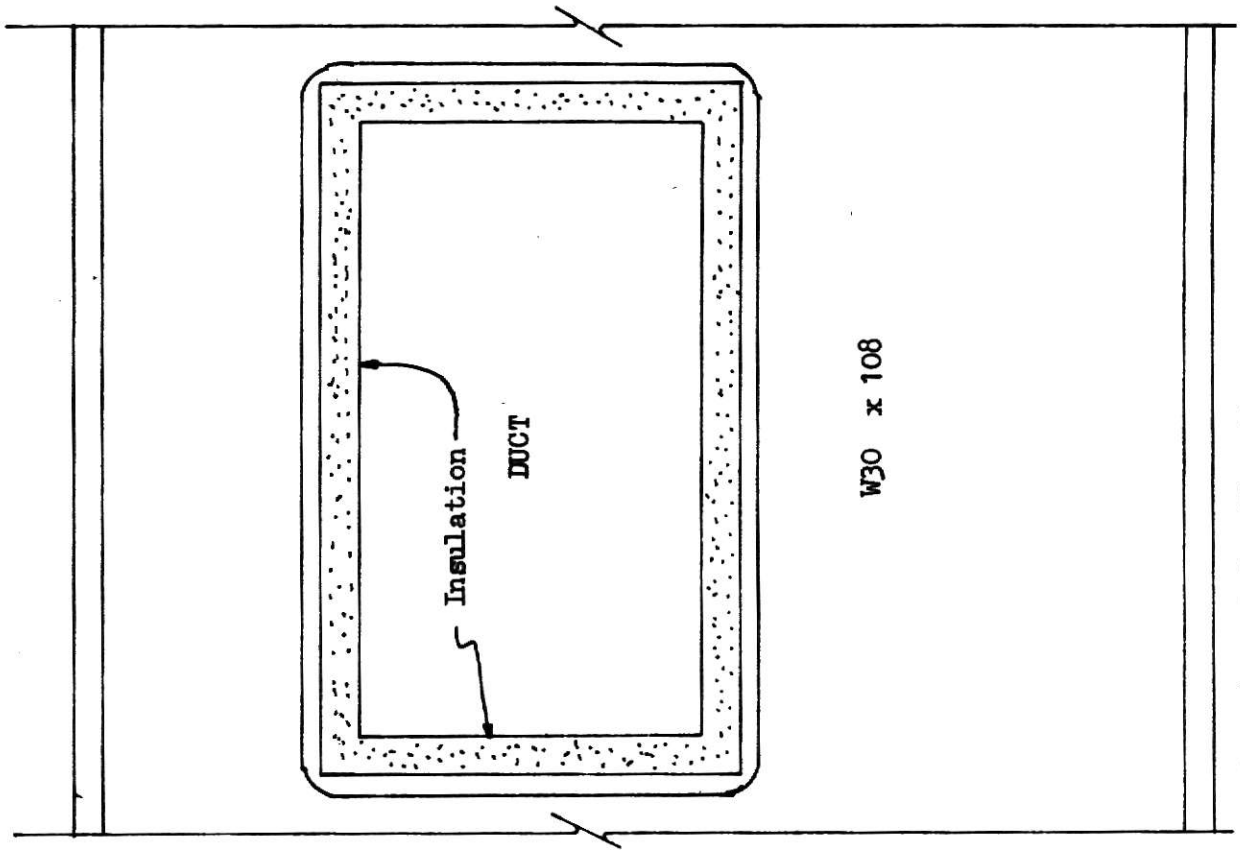

Fig. 14b. Girder Elevation at Opening

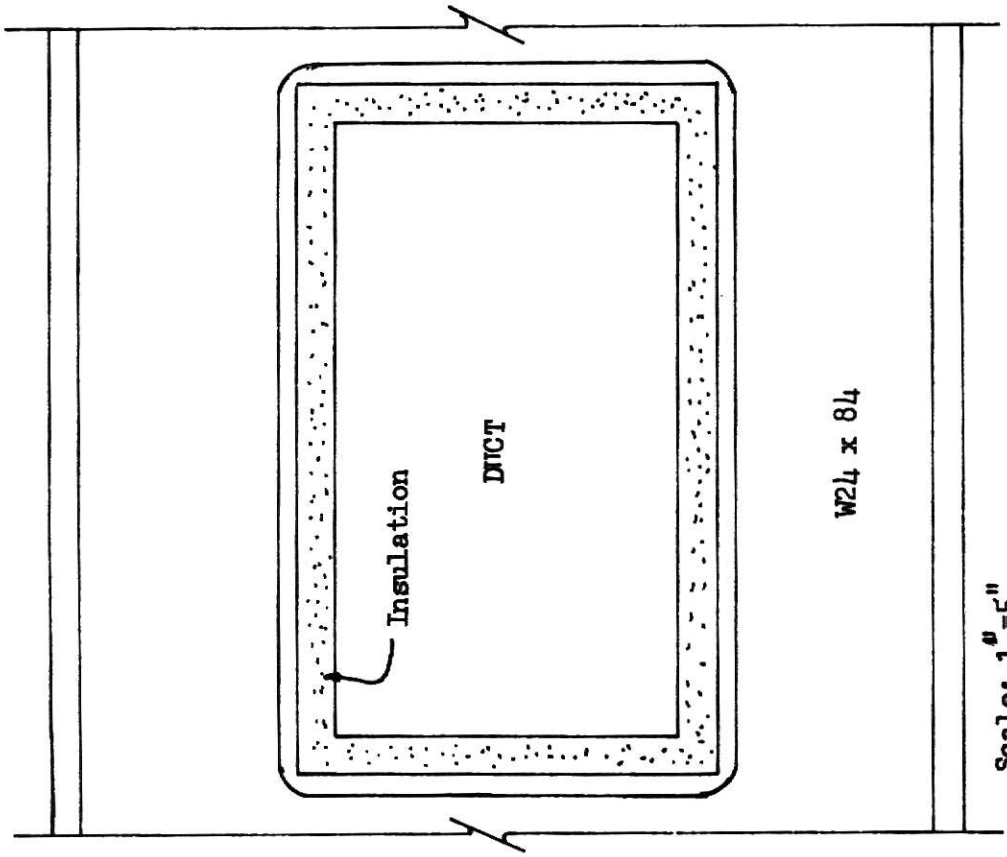

Fig. 14a. Floor Beam Elevation at Opening

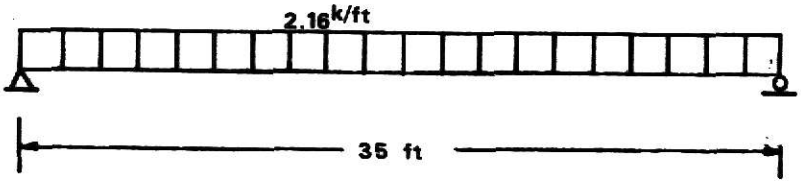

Fig. 15. Floor Beam Loading

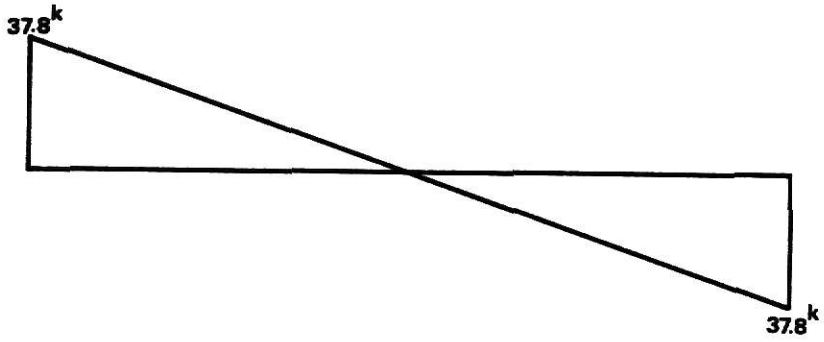

Fig. 16. Floor Beam Shear Diagram

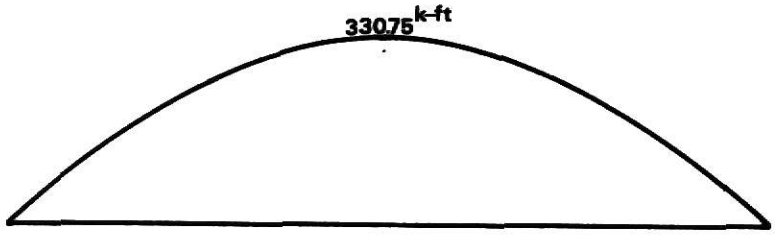

Fig. 17. Floor Beam Moment Diagram

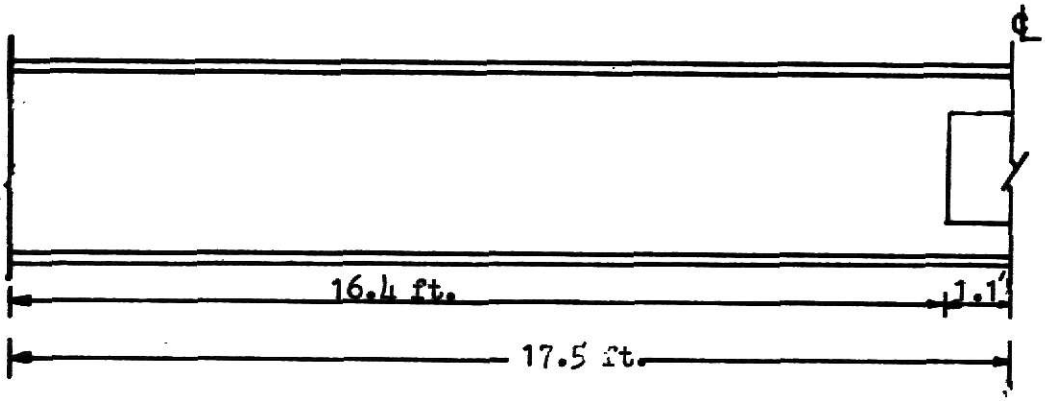

Figure 18a. Permissible Opening Location for Floor Beam with A_r = 0.

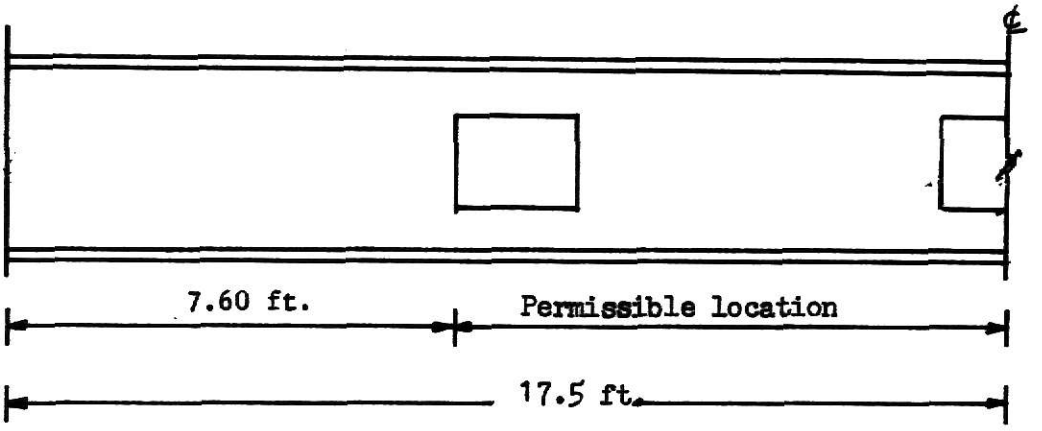

Figure 18b. Permissible Opening Location for Floor Beam with A_r= 0.5 sq.in.

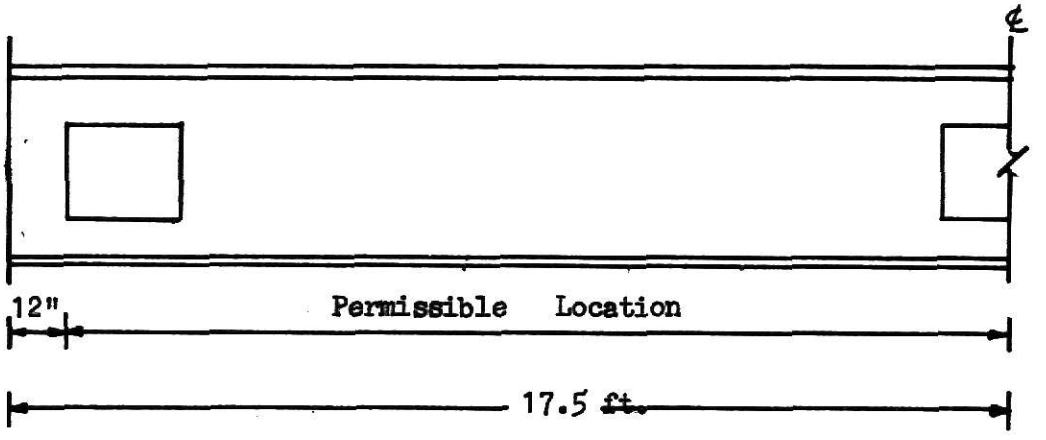

Figure 18c. Permissible Opening Location for Floor Beam with A_r= 1.0 sq.in.

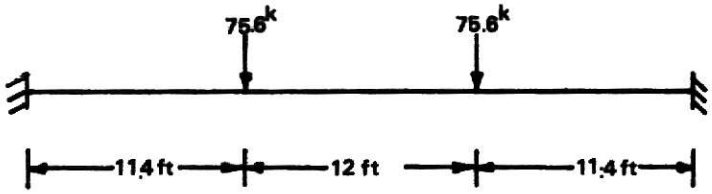

Fig. 19. Girder Loading

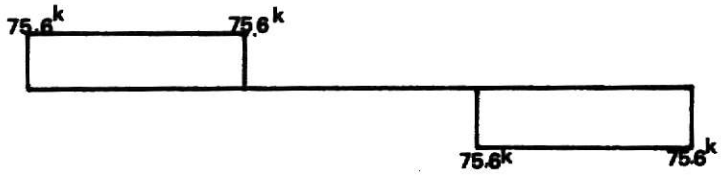

Fig. 20. Girder Shear Diagram

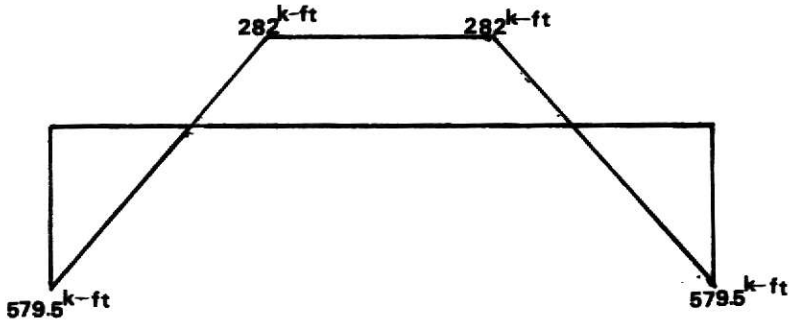

Fig. 21. Girder Moment Diagram

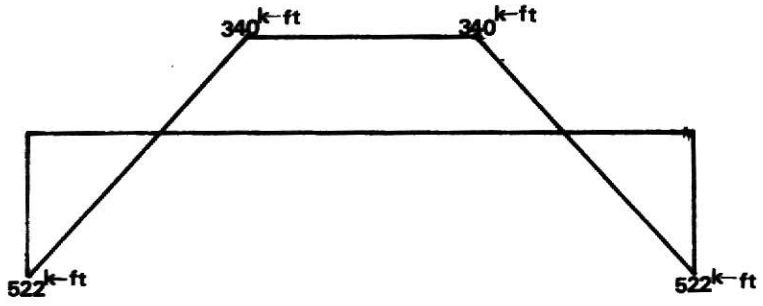

Fig. 22. Girder Moment Diagram with 0.9 Rule

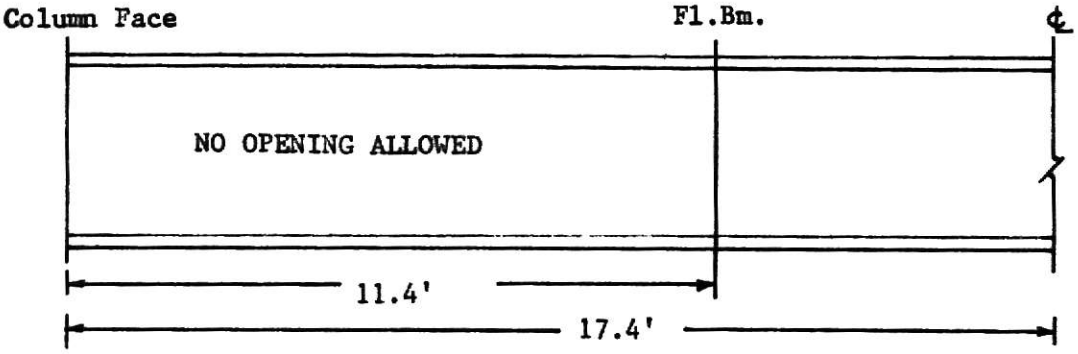

Fig. 23a Permissible Opening Location for Girder with A_r=0.5 sq. in.

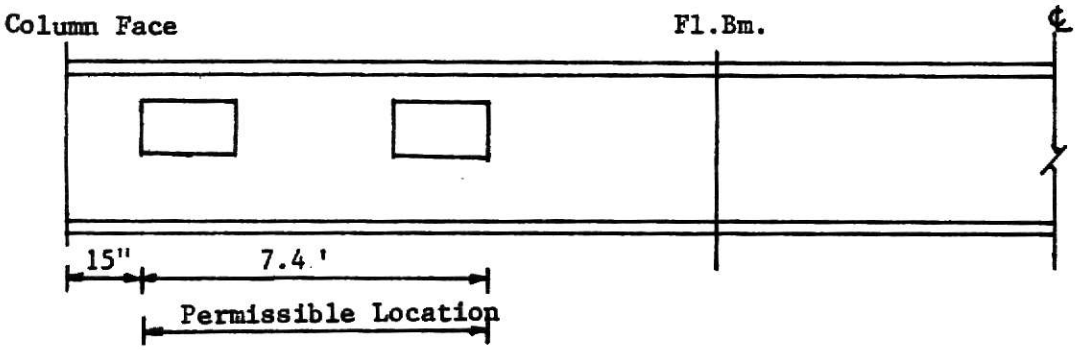

Fig. 23b Permissible Opening Location for Girder with A_r=1.0 sq.in.

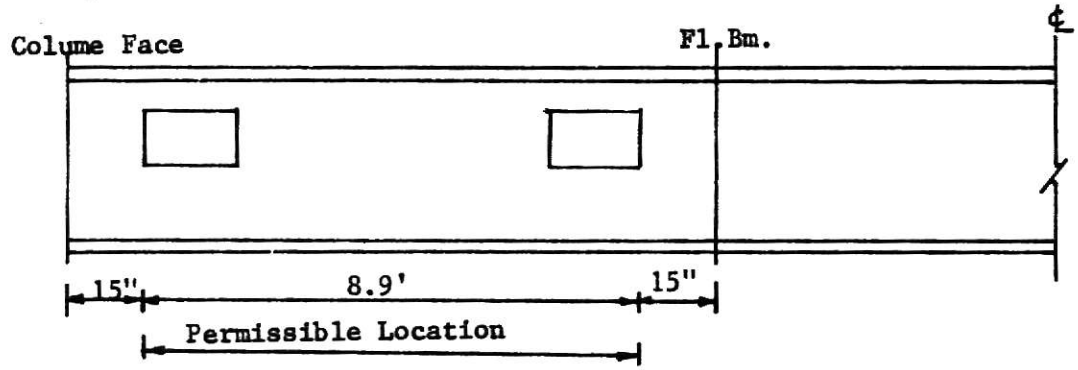

Fig. 23c Permissible Opening Location for Girder with A_r=1.5 sq. in.

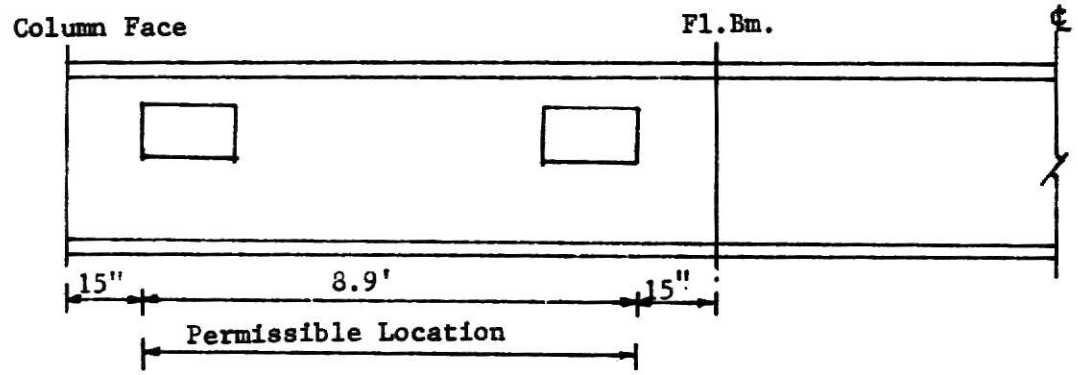

Fig. 23d Permissible Opening Location for Girder with A_r=2.0 sq. in.

DESIGN OF BEAMS WITH ECCENTRIC REINFORCED WEB OPENINGS

by

ROBERT JEN-PING SAND

B.S., National Taiwan University, 1971

AN ABSTRACT OF A MASTER'S REPORT

submitted in partial fulfillment of the

requirements for the degree

MASTER OF SCIENCE

Department of Civil Engineering

KANSAS STATE UNIVERSITY
Manhattan, Kansas

1977

ABSTRACT

In steel buildings it is sometimes necessary to position ducts for heating, ventilation, and air conditioning systems in the same space occupied by the steel beams and girders rather than below these members. For beams of varying depth it is more economical to use eccentric openings in some of the beams than to incorporate numerous vertical bends in the ducts. Usually it is also desirable to add reinforcement to the beam in the vicinity of the web openings instead of using larger sections.

Part I of this report deals with the justification of the Vierendeel Method of Analysis for beams with web opening by comparing experimental data to the theoretical results.

Part II deals with the derivation of the yield equations and the determination of the critical points. Design curves for two specific beams with web openings are constructed.

In Part III the use of the previously developed design formulas and curves for reinforced, concentric and eccentric web openings in steel beams is illustrated with a design example. The example deals with the design of a building floor system consisting of floor beams and girders with different depths.